**RESEARCH ARTICLE**

**Key Points:**

- 10-s reductive leaching is capable of reliably extracting seawater Pb and Nd isotope signals from Southern Ocean sediments
- Natural porewater Pb isotopic compositions are analyzed for the first time in front of the Antarctic Filchner-Rønne Ice Shelf
- Identify potential sites for extracting seawater Pb and Nd isotopic signatures from bulk sediments in the Atlantic sector of Southern Ocean

**Supporting Information:**

- Supporting Information S1
- Data Set S1

**Correspondence to:**

H. Huang,
huanghuang@mail.sysu.edu.cn

# Efficient Extraction of Past Seawater Pb and Nd Isotope Signatures From Southern Ocean Sediments

H. Huang[1] , M. Gutjahr[1] , G. Kuhn[2] , Ed C. Hathorne[1] , and A. Eisenhauer[1]

[1]GEOMAR Helmholtz Centre for Ocean Research Kiel, Kiel, Germany, [2]Alfred-Wegener-Institut Helmholtz-Zentrum für Polar- und Meeresforschung, Bremerhaven, Germany

**Abstract** Radiogenic lead (Pb) and neodymium (Nd) isotope compositions extracted from authigenic phases in marine sediments are sensitive tracers to reconstruct past ocean circulation and water mass mixing. Chemical reductive leaching of hydrogenetic ferromanganese oxyhydroxides from bulk sediments is the most practical way to recover past seawater Pb and Nd isotope signatures in the Southern Ocean, due to the scarcity of alternative archives. However, the leached signal could be compromised if substantial quantities of Pb and Nd were released from non-hydrogenetic sediment fractions during chemical extraction. Here we developed a very short 10-s leaching method to extract reliable seawater Pb and Nd isotope signals from sediments in the Atlantic sector of Southern Ocean. The effect of a previously recommended $MgCl_2$ pre-wash, the role of chelate ligands in the leaching solution and length of leaching time were investigated. The results show that 10-s exposure time of sediments to reductive leaching extracted sufficient and more reliable hydrogenetic Pb and Nd compared with the commonly used 30-min leaching approaches. The robustness of our improved leaching method was validated via direct comparison of Pb and Nd isotope signatures with actual seawater, porewater, and corresponding sediment leachates from three stations in front of the Antarctic Filchner-Rønne Ice Shelf. Our findings also indicate that in contrast previously studied sites on the West Antarctic continental shelf, the bottom seawater Nd concentration is less elevated through benthic fluxes in the area of the southern Weddell Sea shelf.

**Plain Language Summary** Individual modern ocean water masses can often be identified by the isotopic signature of dissolved trace metals lead (Pb) and neodymium (Nd) supplied from surrounding continents. By analyzing past seawater Pb and Nd isotope ratios preserved in the sedimentary archives, we can understand how the ocean circulation changed. In the Southern Ocean, archives preserving past seawater Pb and Nd isotope compositions are very scarce. Thus, the chemical extraction of Pb and Nd from seawater-derived ferromanganese oxyhydroxides within deep marine sediments becomes the most practical way to recover past seawater signal. However, Southern Ocean sediments commonly contain substantial quantities of Antarctic continental fine-grained sediment, which easily partially dissolve during extraction, thereby releasing Pb and Nd, which did not originate from past ambient seawater. Here we established a gentle and efficient extraction method to obtain reliable past Southern Ocean seawater signatures. In addition, via analysis of regional seawater-derived Pb and Nd signatures in the Atlantic sector of Southern Ocean, we found that the sediments further away from Antarctica and volcanically active regions are better suited to preserve unaltered seawater Pb and Nd isotope signals, which strongly supports the unique possibility of tracing past water mass sourcing in the Southern Ocean with our analytical approach.

## 1. Introduction

Radiogenic lead (Pb) and neodymium (Nd) isotope compositions have been successfully applied as sensitive and powerful palaeoceanographic proxies for the reconstruction of past circulation changes and water mass mixing for decades (Burton et al., 1997; Christensen et al., 1997; Foster & Vance, 2006; Frank, 2002; Huang et al., 2020). The radiogenic isotopes $^{206}Pb$, $^{207}Pb$ and $^{208}Pb$ are produced by the decay of $^{238}U$ ($T_{1/2} = 4.47$ Ga), $^{235}U$ ($T_{1/2} = 707$ Ma), and $^{232}Th$ ($T_{1/2} = 14$ Ga), while the radiogenic isotope $^{143}Nd$ is also produced by a very slow α-decay of $^{147}Sm$ ($T_{1/2} = 106$ Ga). Because of these long half-lifes, crustal radiogenic/primordial isotopes ratios, i.e. $^{206}Pb/^{204}Pb$ and $^{143}Nd/^{144}Nd$ (commonly expressed in $\varepsilon_{Nd} = [(^{143}Nd/^{144}Nd)/0.512638-1]\times10^4$), are constant on relatively short Cenozoic timescales unless crustal reservoirs were mixed. Dissolved Pb and Nd in the oceans are mainly supplied by continental runoff, so Pb and Nd isotope signatures of the water masses

are determined by the average regional crustal compositions of weathered continental crust. Substantial quantities of dissolved Nd are also delivered to the oceans by sediment-bottom water exchange along continental margins (Lacan & Jeandel, 2005; Lacan et al., 2012; Pöppelmeier et al., 2020; Rempfer et al., 2011) or oceanic islands (Pearce et al., 2013; Rempfer et al., 2011; Stichel, Frank, Rickli, Hathorne, et al., 2012). However, to date such a mechanism has not been reported for seawater Pb. This is (i) because of difficulties in acquiring reliable seawater Pb concentration data, and (ii) because Pb released from continental margin sediments is very likely efficiently re-adsorbed within sedimentary porewaters due to its high particle-reactivity. The average oceanic Nd residence time between 600 and 2000 years (Tachikawa et al., 2003, 1999), more recent estimates below 500 years (Arsouze et al., 2009; Siddall et al., 2008), allows $\varepsilon_{Nd}$ to serve as a quasi-conservative water mass tracer away from ocean margins. In contrast to Nd, Pb has a much shorter residence time (50–200 years) (Cochran et al., 1990; Henderson & Maier-Reimer, 2002; Schaule & Patterson, 1981), allowing it to track local and generally rather proximal weathering inputs (Crocket et al., 2013, 2012; Gutjahr et al., 2009; Kurzweil et al., 2010).

Various archives have been successfully employed to recover seawater Pb and Nd isotope signals in the past, such as fossil fish teeth/debris, fossil foraminifera, Fe-Mn crusts or nodules, sedimentary ferromanganese (Fe-Mn) oxyhydroxides, and cold-water corals. In very early studies, extracting past seawater Pb and Nd isotope signals were mainly conducted using Fe-Mn crusts (Abouchami et al., 1997; Burton et al., 1997; Belshaw et al., 1998; Frank et al., 2002; O'Nions et al., 1998; Reynolds et al., 1999; van de Flierdt et al., 2004). However, due to its slow growth rate, Fe-Mn crusts are not suitable for generating records of (sub-) millennial resolution. Fossil fish teeth (Martin & Scher, 2004; Staudigel et al., 1985) and fossil foraminifera (Klevenz et al., 2008; Roberts et al., 2010; Vance & Burton, 1999) in marine sediments are both reliable archives for (sub-) millennial resolution seawater Nd isotope studies. However, fossil fish debris was found not to be suitable for Pb isotopic reconstructions (Basak et al., 2011). In addition, fossil foraminifera and fish debris are often not available in sufficient quantities for a hydrogenetic Nd isotope reconstruction of high precision and desired temporal resolution, especially in deep Southern Ocean sediments which are often carbonate-free. Cold-water corals represent a good alternative because their age can be well constrained. Nevertheless, only recently cold-water corals were shown to be a robust archive both for extracting seawater derived Pb (Lee et al., 2014, 2017; Wilson et al., 2017) and Nd (Colin et al., 2010; Struve et al., 2017; van de Flierdt et al., 2006; Wilson et al., 2014). However, fossil cold-water corals are usually not found in situ in abyssal water depths below the aragonite or calcite compensation depths. Furthermore, the extraction of coral-hosted Nd or Pb is complex and multi-millennial continuous temporal coverage is often not achievable. Past seawater Pb and Nd isotope reconstructions generated via reductive leaching of sedimentary Fe-Mn oxyhydroxides in bulk sediments has also been established as a robust procedure in various deep marine settings (Blaser et al., 2016; Gutjahr et al., 2007; Martin et al., 2010). Since Southern Ocean sediments usually do not contain sufficient biogenic components, reductive leaching is so far the only practical option to extract deep sea Pb and Nd isotope signal in deep marine high latitude settings, which has also been successfully applied in carbonate-free Arctic sediments to obtain a reliable bottom water Pb and Nd signal (Chen et al., 2012; Haley et al., 2008).

The previously reported reductive leaching methods for extracting authigenic Pb and Nd isotope signatures from marine sediments are slightly different from each other so some issues need to be addressed before the establishment of a refined extraction method for authigenic Fe-Mn oxyhydroxide-sourced Pb and Nd. The first is whether it is necessary to pre-wash a sediment sample with $MgCl_2$ solution. The $MgCl_2$ pre-wash was proposed to remove potentially present contaminating phases prior to reductive Fe-Mn oxyhydroxide leaching. This technique was introduced decades ago (Tessier et al., 1979) and especially used for leaching sedimentary seawater-derived Pb (Gutjahr et al., 2009, 2007). However, no study has as yet assessed the necessity of carrying out a $MgCl_2$ pre-wash from an isotopic perspective. Second, chelate ligands, like EDTA, were used in reductive leaching to prevent re-adsorption of released authigenically sourced trace metals (Blaser et al., 2016; Chen et al., 2012; Gutjahr et al., 2007), but many other studies did not add chelate ligands to their leaching reagents (Basak et al., 2011; Du et al., 2016; Haley et al., 2008; Wilson et al., 2013). The benefit of adding EDTA is to prevent re-adsorption via complexation of dissolved authigenic Pb (Gutjahr et al., 2007), yet whether adding ligands into the leaching solution may introduce contamination or cause undesired isotopic fractionation is as yet untested. In more recent studies, 30 min exposure time of sediments to chemical reagents was usually recommended as a suitable leaching time, without prior
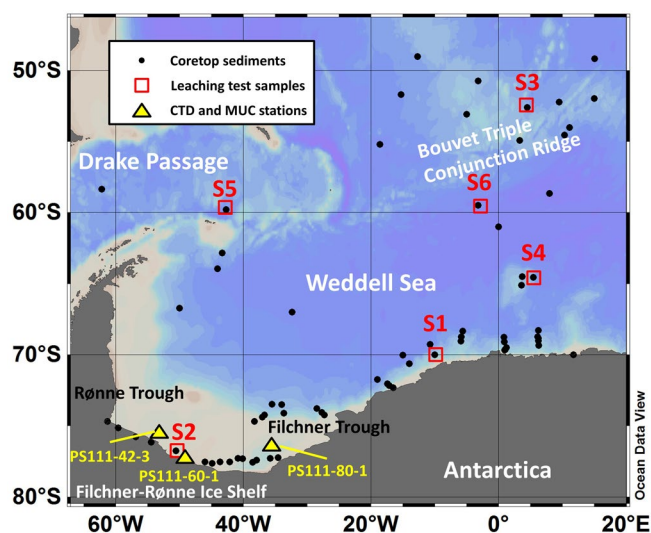
**Figure 1.** The locations of sample sites used in this study.

chemical carbonate removal (Blaser et al., 2016; Du et al., 2016; Wilson et al., 2013). Since shorter leaching time should dissolve less material from the non-hydrogenetic fraction, a very short contact time, i.e. 10 s, should theoretically extract even purer hydrogenetic Pb and Nd isotope signals than 30 min leaching, especially for Southern Ocean sediments which commonly contain substantial quantities of only physically weathered continental detritus that is particularly susceptible for unwanted rare earth element (REE) release during chemical extraction (Diekmann et al., 2003; Diekmann & Kuhn, 1999; Michels et al., 2002; Middelburg et al., 1988; Yusoff et al., 2013).

In this study, we investigated the effects of $MgCl_2$ pre-wash, presence or absence of chelate ligands and leaching time on extracted authigenic Nd and Pb isotope compositions in the Atlantic sector of Southern Ocean in order to optimize the leaching method. Since the ability that chemical extraction of sedimentary Fe-Mn oxyhydroxides can extract seawater Pb and Nd isotope signals is debated (Bayon et al., 2004; Haley et al., 2004), we also analyzed Pb and Nd isotopic compositions in seawater, porewater, and leachates at three sampling stations in the front of Filchner-Rønne Ice Shelf in the southernmost accessible Weddell Sea area. The suggestion that sediment-derived Nd is a dominant source for the global oceanic Nd budget (Arsouze et al., 2009; Rempfer et al., 2011; Tachikawa et al., 2003) is revisited for the southern Weddell Sea. Furthermore, we generated Pb and Nd isotopic maps via analysis of 70 core top sediment samples in the Atlantic sector of the Southern Ocean for a better understanding of the interaction between sediments and seawater in different geologic settings. These maps also allow identification of most suitable sediment core sites for palaeoceanographic studies.

## 2. Materials and Methods

### 2.1. Sample Sites

The locations of seawater, sedimentary porewater, and sediment samples used in this study are shown in Figure 1. Seventy core top sediment samples were collected from the Alfred-Wegener-Institute Core Repository in Bremerhaven (Germany) for leaching tests and regional mapping of sedimentary seawater-derived Nd and Pb isotopic compositions in the Atlantic sector of the Southern Ocean. Seawater samples for Pb and Nd isotope analyses were taken from three stations in front of the Filchner-Rønne Ice Shelf using Niskin bottles mounted onto a CTD-rosette during expedition PS111 from January to March 2018 onboard RV Polarstern. Porewater and sediment samples were also retrieved at these three stations by multicore (MUC) sampling during the same cruise.

### 2.2. Leaching Experiments

Although chemical reductive leaching has been applied to extract trace metals from marine Fe-Mn oxyhydroxides since the 1960s (Chester & Hughes, 1967), it is still under development to date. One major concern is that the leaching solution applied in the procedure inevitably dissolves both hydrogenetic fractions and non-hydrogenetic sediment components, such as continental detritus and volcanic ash, potentially contaminating the seawater-derived signal. There are two effective ways to minimize contamination: 1) using weak/diluted leaching solution and 2) short leaching time (Blaser et al., 2016; Chen et al., 2012; Gutjahr et al., 2007; Wilson et al., 2013). A smaller solution/solid ratio was also suggested to be an option to reduce contaminations (Wilson et al., 2013). In principle, the leaching reaction consumes chemicals, like hydroxylamine hydrochloride, in the leaching solution and a lower solution/solid ratio therefore result in a less aggressive leaching solution. Based on these two principles, a revised leaching procedure has been recently presented for the gentle extraction of a porewater Nd isotopic signature from bulk sediments in the Atlantic Ocean (Blaser et al., 2016). In the following, we refined this method to extract both seawater-derived Pb and Nd from Southern Ocean sediments. Furthermore, we investigated (i) the effect of the $MgCl_2$ pre-wash,
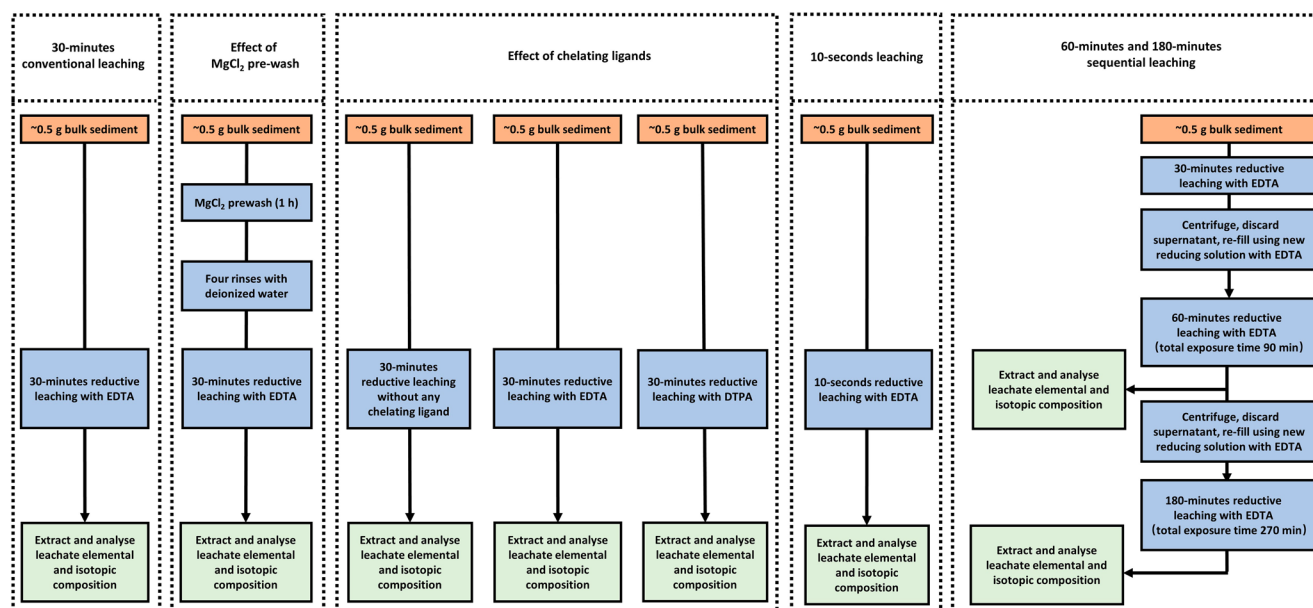
**Figure 2.** Schematic view of conventional and control leaching experiments.

which was proposed to remove potentially present exchangeable contaminations (Gutjahr et al., 2007; Tessier et al., 1979), and (ii) the effect of chelate ligand used to prevent re-adsorption.

Six core top sediment samples, named from S1 to S6 (Table S1), were selected for sequential leaching tests from different locations in the Atlantic sector of the Southern Ocean (Figure 1). The NOD-A-1 powder, a pure Fe-Mn oxyhydroxide nodule standard provided by the USGS, was used as a reference material (S7). The latest previously published leaching procedure (Blaser et al., 2016) described below was used as the analytical protocol to be modified:

### 2.2.1. Conventional Leaching

Approximately 0.5 g of wet bulk sediment or 0.05 g reference material was weighed in prior to chemical extraction. The weighed samples were agitated in 15 mL leaching solution for 10 s on a vortex shaker to suspend the sediment and then in a regular shaker for 30 min. After centrifugation, 6 mL of the leachate was pipetted out for concentration and isotope analysis. The leaching solution contained 0.005 M hydroxylamine hydrochloride (HH), 1.5% acetic acid and 0.001 M EDTA buffered to pH~4 with suprapure NaOH (corresponding to a final molarity of ~0.033 M NaOH) in acid-cleaned polypropylene 50 mL centrifuge tubes. This leaching solution is a diluted version of a previously used reductive leaching solution protocol (Gutjahr et al., 2007). The buffering solution NaOH could also be replaced with suprapure ammonia (cf. Blaser et al., 2019), yet we did not employ this reagent here.

Following the conventional leaching protocol, a series of control leaching experiments (Figure 2) were carried out on separate set of samples (S1–S7) as follows:

1. *Effect of MgCl₂ pre-wash:* before conventional leaching, aliquoted sediment samples were mixed with 20 mL 1 M MgCl₂ solution for 1 h in a shaker. After centrifugation at 2,500 rpm and decanting of the supernatant, the samples were washed four times with 35 mL Milli-Q® grade deionized water, followed by centrifugation for 5 min at 3,000 rpm and decanting of the supernatant
2. *Effect of chelating ligands:* Two different leaching solutions were modified from conventional leach solution: one used diethylenetriaminepentaacetic acid (DTPA) to replace EDTA and another without chelating ligands inside. Separate sediment aliquots were processed using the conventional 30-min leaching method with these two different leaching solutions
3. *10-s leaching:* separate sediment aliquots were only exposed to leaching solution for 10 *s* on the vortexing shaker without further 30 min leaching in the regular shaker

4. *60-min and 180-min sequential leaching:* after 30 min conventional leaching and extraction of leachate solutions, the remaining supernatants were discarded and replaced with 15 mL of new leaching solution. Sediments were then left to react for 60 min extended leaching on a shaker and the leachates were again collected for analysis. Following centrifugation, removal of the supernatant, another 15 mL of new leaching solution was added to the sample residues to leach for another 180 min on a shaker and this last leachate fraction was subsequently collected too. Overall, the cumulative sediment exposure time during extended leaching experiments including the 60 min and 180 min sequential leaching steps are hence 90 min and 270 min, respectively. Together with the separately collected 10-s and 30-min leach fractions this results in a total of four individual leach aliquots using EDTA as chelating reagent per sample (S1–S7). The leaching experiment data are presented in Tables S2–S4

### 2.3. Seawater Pb and Nd

The best way to validate a leaching method is to directly compare the actual seawater isotope signal with corresponding leachate isotopic compositions. Unfortunately, the modern-day natural seawater Pb is entirely contaminated by anthropogenic sources but a very recent study showed that seawater very close to Antarctica is still relatively unaffected containing about 95% natural Pb (Ndungu et al., 2016). This suggests that seawater Pb in remote Antarctic ocean basins protected under sea ice should be more pristine than anywhere else. Therefore, we sampled seawater at around 76°S on the Antarctic shelf in front of Filchner-Rønne Ice Shelf for Pb and Nd isotope analysis (Figure 1) where seawater is covered by sea ice during most of the year.

Shelf seawater samples used in this study were collected from different depths in the water column using Niskin bottles mounted on a stainless steel CTD rosette and MUC for shelf bottom water. In order to distinguish seawater sampled by CTD and MUC, we denote these as CTD seawater and MUC bottom water, respectively. While seawater sampling for Nd isotopic analyses are commonly undertaken using this seawater sampling approach, for seawater Pb collection usually trace metal-clean approaches are necessary (Rijkenberg et al., 2015). Since such a sampling device was not available during PS111, potential Pb contamination is a concern. The Pb contamination issue is discussed later in Section 4.1.

The seawater samples were filtered through a 0.2/0.8 μm Acropak® filter and then acidified to pH ∼2 using double distilled concentrated nitric acid. From each depth, ∼10–20 L seawater was collected in acid-cleaned 20 L LDPE-collapsible cubitainers for Nd isotopes analysis, 1 L seawater was collected in acid-cleaned 1 L PE bottle for Pb isotope analysis and 250 mL seawater sample was collected in acid-cleaned 250 mL PE bottles for Pb and Nd concentration measurements. Besides the large volume seawater samples for Nd isotope analysis, all other samples were only filtered and acidified on board and further processed in the GEOMAR Kiel (Germany) clean laboratory facilities.

The ∼10–20 L seawater samples for Nd isotopic analysis were further processed on board by adding purified dissolved Fe–chloride solution. After 6 h equilibration time, ammonia solution (25%, Merck suprapur®) was added to raise the pH to 7.5–8.5 in order to co-precipitate dissolved Nd with iron oxyhydroxides. After settling of the precipitates, most of the supernatant was discarded and the residue was transferred into 1 L acid-cleaned PE-bottles for transport to the home laboratory.

After transport to the clean room facilities at GEOMAR Kiel, the iron oxyhydroxide precipitates were transferred into acid-cleaned 50 mL centrifuge tubes and centrifuged for 10 min at 4,000 rpm. Subsequently samples were rinsed at least two times with Milli-Q® grade deionized water followed by centrifugation to wash out major ions (Ca, Mg, K, etc.). The precipitates were dissolved in 2 mL 6 M HCl and transferred into 30 ml Teflon vials to dry down on the hotplate. Subsequently, 2 mL aqua regia (HNO$_3$: HCl = 1:4) was added, refluxed for 24 h and afterward dried down. Then 2 mL of 6 M HCl was added and dried down again to transfer back to Cl-form. Before column purification, the excess amount of Fe is separated from the sample via Fe back extraction. For this step, each dried sample was re-dissolved in 4 ml of 6M HCl and mixed with a suitable amount (about 3 mL) cleaned di-ethyl ether (Stichel, Frank, Rickli, & Haley, 2012). About 90% of dissolved iron can be extracted into the organic solution phase and discarded. This Fe-extraction procedure was repeated twice or more often until the sample solutions became pale yellow. After evaporation,

the seawater samples were re-fluxed in 2 ml 6M HCl and dried down again before the subsequent cation exchange purification step.

The extraction of Pb from CTD seawater, as well as Pb and Nd from MUC bottom water, was equally operated in the home clean laboratory. 5 mL of concentrated ammonia solution (25%, Mercksuprapur®) was added into 1 L acidified seawater samples to raise the pH to 10. After 2 days of reaction time, white $Mg(OH)_2$ precipitates slowly formed. The supernant was then discarded and the white residue dissolved in 6 mL 2M HBr/0.1 M HF solution for further ion chromatographic Pb and Nd purification. All seawater Pb and Nd isotope data are listed in Table S5.

### 2.4. MUC Sediment and Porewater

All operations for porewater sampling from MUC sediments were undertaken in a glove bag under oxygen-free conditions in an argon gas atmosphere. The acid-cleaned centrifuge tubes and sample bottles were also flushed with argon gas before use. After extraction of overlying seawater via siphoning, the MUC sampling tube was transferred into the glove bag and MUC sediment was sampled in 2 cm increments on a Teflon sampling stand. Each 2 cm sub-sample was transferred in a 50 mL centrifuge tube. The porewater was separated from sediment by centrifugation at 4,000 rpm for 60 min. Consequently, the porewater was filtered through a pre-cleaned 0.2 μm Supor®filter and acidified to pH∼2. About 10–20 mL porewater samples were recovered from each depth from one sample tube. The remaining sediment samples were frozen and kept for reductive leaching experiments. All samples were transported back home for further chemical purification and isotope measurements at GEOMAR Kiel. Prior to further treatment in the clean laboratory, the porewaters remained in argon gas atmosphere conditions in the sample bottles.

Dissolved Pb contained in sediment porewaters was directly dried down for Pb column purification without any additional treatment in order to minimize potential blank contributions. Authigenic Pb in the remaining MUC sediment samples was extracted using the 10-s leaching method (detailed in Section 2.2) before purification by ion chromatography. The MUC sediment leaching and porewater data are presented in Table S6.

### 2.5. Authigenic Pb and Nd Isotopic Core Top Sediment Mapping

A total of 70 core top sediment samples were processed using the 10-s leaching method described in Section 2.2 for the generation of authigenic Pb and Nd isotopic maps of the Atlantic sector of the Southern Ocean. The Pb and Nd aliquots were purified by ion chromatography. The data of Pb and Nd isotopic map are available within the Pangaea data base (DOI: https://doi.pangaea.de/10.1594/PANGAEA.924604)

### 2.6. Ion Chromatography

The Pb cuts in the porewater and leachates were purified by ion chromatography on miniaturized columns containing ∼80 μL AG1-X8 resin (Lugmair & Galer, 1992). The MUC bottom water and CTD seawater Pb cuts, which were pre-concentrated using the $Mg(OH)_2$ co-precipitation method, can form substantial quantities of silicate gel and clog the column during normal Pb chromatography. In order to dissolve the silicate gel, 6 mL 2 M HBr/0.1 M HF was added to the $Mg(OH)_2$ precipitate from each 1 L seawater sample. The protocol (Table S7) used to purify Pb is modified from an earlier study (Paul, Bridgestock, et al., 2015). After Pb purification, the remaining REE cuts were separated by cation exchange chromatography using 50W-X8 resin followed by separation of Nd from the other REE using LN-Spec resin (Cohen et al., 1988).

### 2.7. Mass Spectrometry

Element concentrations were measured with an Agilent 7500-CE Quadrupole ICP-MS at GEOMAR Kiel. Two different standard calibrations were employed to cover samples of high and low trace element concentrations with reproducibility strongly dependent on the respective element. All concentration results were normalized to the initially used sample weight (in μg/gram of wet bulk sediment weighed in).

Seawater Pb and Nd concentration measurements were conducted on a 7 mL sample loop using an online pre-concentration technique (OP) ICP-MS at GEOMAR employing an automated "SeaFast" system

(Elemental Scientific Inc.) coupled to a Thermo Scientific Element XR. The Pb and Nd concentration was analyzed with the same established method used for REE concentration measurements (Hathorne et al., 2012). During measurements, the GEOTRACES seawater reference Bermuda Atlantic time series (BATS) 15 m and the BATS 2,000 m (MF-20) (van de Flierdt et al., 2012) together with the Cape Basin deep water inhouse reference were used to assess the reproducibility and accuracy of the data (see Table S5).

Pb and Nd isotope measurements were performed on a Thermo Scientific Neptune Plus MC-ICP-MS at GE-OMAR, Kiel. Mass bias correction during Pb isotope measurements was done externally using the Tl-doping technique (Belshaw et al., 1998; Süfke et al., 2019) with added NIST997 Tl standard solution. Given that Tl and Pb fractionate slightly differently during ionization, $^{205}$Tl/$^{203}$Tl were determined on a session-by-session basis so that NBS981 Pb isotope compositions matched published compositions (Baker et al., 2004; Süfke et al., 2019; Thirlwall, 2002). Total Pb procedural blanks in leachates and seawater samples were below 50 pg ($n = 30$) and are hence negligible. The total Pb procedural blanks in porewater were below 2 pg ($n = 2$) and the sample were between 50 and 100 pg, so the blank Pb contaminations were lower than 4%. The reproducibility of the secondary standard USGS NOD-A-1 is listed in Table S8. As shown in the table, all measured standard Pb isotopic ratios are within the error of published compositions. The 2 SD of the secondary standard USGS NOD-A-1 are used to indicate the error bars of measured Pb isotopic ratios in all figures.

Instrumental mass fractionation during Nd isotopic analyses was corrected by normalizing the measured ratio of $^{143}$Nd/$^{144}$Nd to $^{146}$Nd/$^{144}$Nd = 0.7219 and $^{142}$Nd/$^{144}$Nd = 1.141876 using the mass bias correction procedure of Vance and Thirlwall (2002). The measured Nd isotope ratios were normalized to the published $^{143}$Nd/$^{144}$Nd value of 0.512115 for JNdi-1 (Tanaka et al., 2000). Total procedural blanks for Nd are below 30 pg and hence negligible ($n = 20$). Secondary standard solution NIST 3135a was run with the samples to check the external reproducibility. The secondary standard NIST 3135a reproduced within 0.2 $\varepsilon_{Nd}$ for a 50 ppb solution ($n = 169$, 2 SD), and 1.25 $\varepsilon_{Nd}$ for a 2 ppb concentration ($n = 5$, 2 SD; see Table S9). The 2 SD of the secondary standard NIST 3135a are employed to illustrate the reproducibility precision of measured Nd isotopic compositions in all figures.

## 3. Results

### 3.1. Effect of MgCl$_2$ Pre-wash

The Pb isotopic compositions of MgCl$_2$ pre-washed samples were all either identical within error or less radiogenic (lower) in $^{206}$Pb/$^{204}$Pb and $^{208}$Pb/$^{204}$Pb compared to the samples processed without MgCl$_2$ pre-wash (Figure 3a and 3c). Only sample (S1) was not affected by MgCl$_2$ pre-wash. In contrast to the obtained Pb isotopic results, Pb concentrations recovered by these two approaches were almost identical. On the other hand, both $\varepsilon_{Nd}$ and Nd concentrations extracted from all samples are within error both with or without preceding MgCl$_2$ pre-wash (Figure 3d).

### 3.2. Effect of Chelate Ligand

Leaching solutions containing EDTA and DTPA had a much higher Pb and Nd recovery rate than solutions without ligands (Figure 4). This result clearly shows that the lack of chelating ligands in the leaching solution leads to pronounced Pb and Nd re-adsorption during chemical extraction. Between the two tested ligands, EDTA shows a stronger complexation ability both toward Nd and Pb than DTPA. Although ligands have a strong influence on the Pb and Nd recovery rate, all $\varepsilon_{Nd}$ values and most $^{206}$Pb/$^{204}$Pb, $^{208}$Pb/$^{204}$Pb and $^{207}$Pb/$^{206}$Pb ratios produced from these samples are identical within error, indicating that the addition of ligands neither introduces contamination nor causes isotopic fractionation. Only $^{208}$Pb/$^{204}$Pb of S2 and all displayed Pb isotopic ratios in S4 leachates produced divergent results as a function of chelating reagent used.

### 3.3. Effect of Leaching Time

A wide range of treatment times, from 10 s to a total of 270 min (30 + 60 + 180 min), was investigated for all samples. The Pb and Nd isotopic compositions sequentially leached out from the USGS NOD-A-1
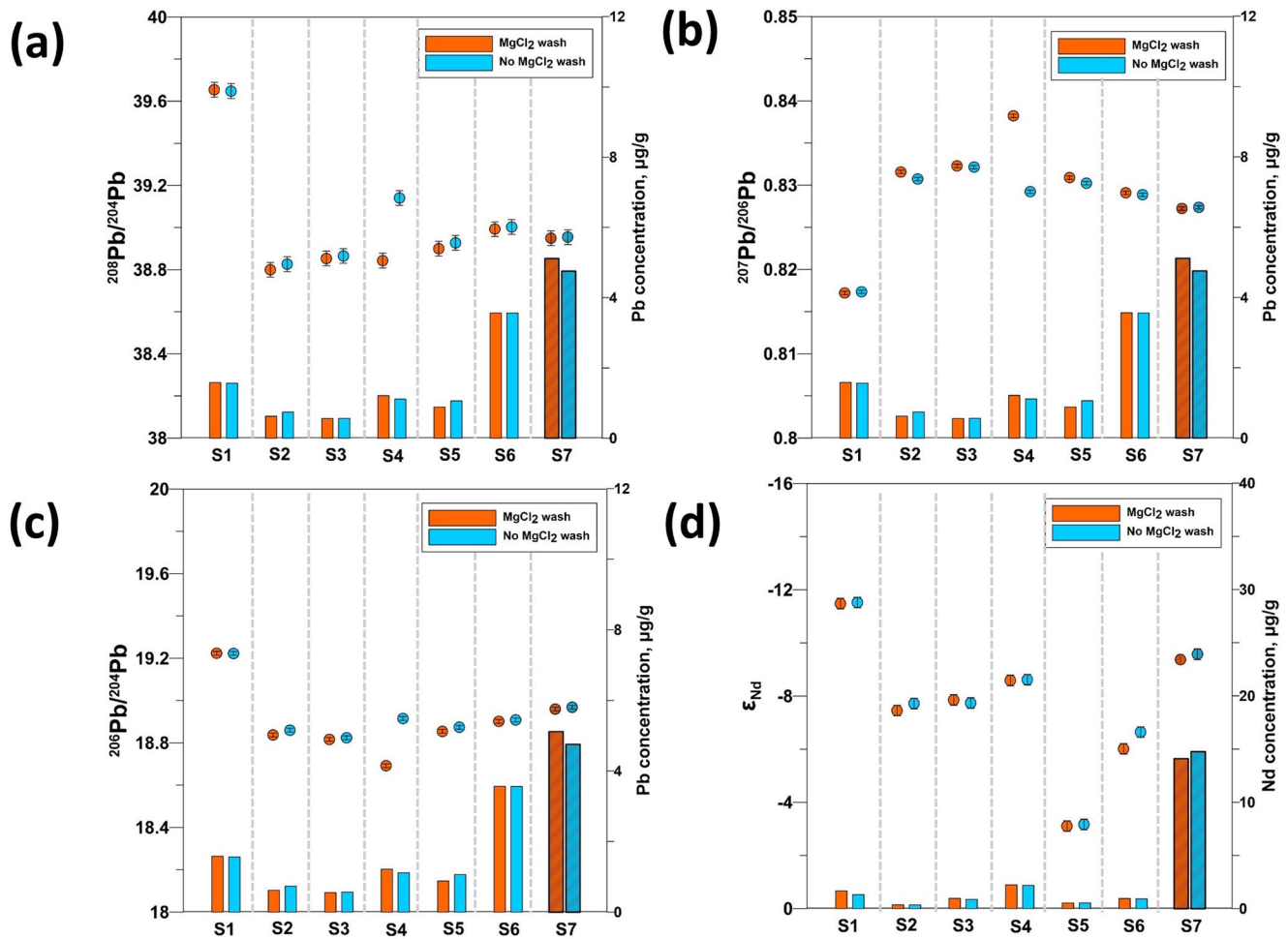
**Figure 3.** Effect of $MgCl_2$ pre-wash. Round dots indicate isotopic compositions and bar charts indicate recovery concentrations in the leachates. (a) $^{208}Pb/^{204}Pb$ and Pb concentration. (b) $^{207}Pb/^{206}Pb$ and Pb concentration. (c) $^{206}Pb/^{204}Pb$ and Pb concentration. (d) $\varepsilon_{Nd}$ and Nd concentration. The results conducted by USGS NOD-A-1 standard (S7) are highlighted with stippled bar charts.

standard are obviously invariant, because it is a largely homogeneous Fe-Mn oxyhydroxide-based material. $^{206}Pb/^{204}Pb$ and $^{208}Pb/^{204}Pb$ in the sediment leachates were generally increasing and $^{207}Pb/^{206}Pb$ were decreasing with extended leaching time. Sediments from sites S1, S2, and S4 which were sampled close to the Antarctic continent showed the most pronounced offsets with increasing leaching time. In contrast, sequential leaching had only little or no impact on Pb isotope signatures of the samples, S3, S5, and S6 that were derived from deep open ocean locations (Figures 1, 5a, 5b, and 5c). Similar to Pb isotopic compositions, $\varepsilon_{Nd}$ values in sediment leachates also shifted toward more radiogenic (higher) values from 10 s to a total of 90 min exposure time but reversed to less radiogenic (lower) values or increased to very high $\varepsilon_{Nd} > 0$ of S3 in the last 180 min sequential leaching duration of the total 270 min, indicating that the prolonged leaching minutes targeted different sediment fractions with distinct $\varepsilon_{Nd}$ compositions (Figure 5d), while the easily extractable Fe-Mn oxyhydroxides were already removed during earlier leaching stages.

### 3.4. Filchner-Rønne Shelf Seawater Pb and Nd

Generally, as shown in Figure 6, the seawater Pb and Nd concentrations in the three CTD and MUC stations along the Filchner-Rønne Ice Shelf increase with increasing water depth. As evident from Figure 7, seawater Pb concentrations collected by CTD at these three stations from cruise PS111 match the seawater Pb concentration range sampled in previous studies using trace metal clean devices at nearby GEOTRACES
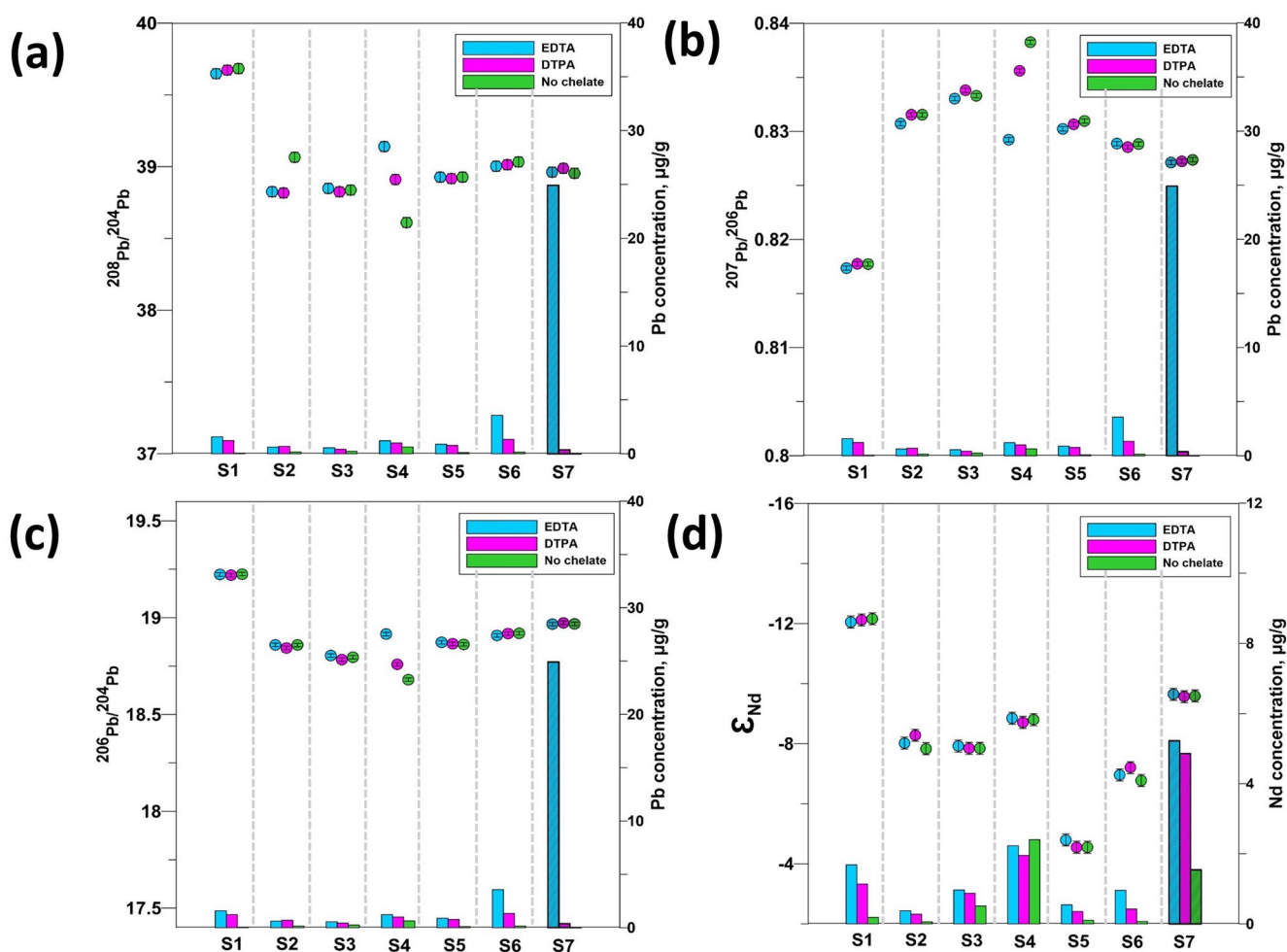
**Figure 4.** Effect of chelating ligands. Round symbols illustrate Pb isotopic compositions or $\varepsilon_{Nd}$ in the leachates; Bar charts show Pb or Nd concentration values in the leachates. (a) $^{208}Pb/^{204}Pb$ and Pb concentration. (b) $^{207}Pb/^{206}Pb$ and Pb concentration. (c) $^{206}Pb/^{204}Pb$ and Pb concentration. (d) $\varepsilon_{Nd}$ and Nd concentration. The results conducted by USGS NOD-A-1 standard (S7) are distinguished with stippled bar charts.

stations (Lee et al., 2015; Schlitzer et al., 2018), while Pb concentrations collected by MUC are extremely high indicating an anthropogenic contamination. The Nd isotope compositions of Filchner-Rønne shelf seawater showed remarkably little deviation from an average $\varepsilon_{Nd} = -9.25 \pm 0.35$ (2 SD), which agree with published Weddell Sea Deep and Bottom Water $\varepsilon_{Nd}$ signatures further north between $-8.4$ and $-9.6$ (Stichel, Frank, Rickli, & Haley, 2012). The seawater $^{206}Pb/^{204}Pb$ ratios of CTD station PS111_80-1 increase from 18.18 to 18.72 with increasing water sampling depth. This station also shows a quasi-linear increase of Pb concentrations with water depth from 10.1 pmol/kg in 20 m water depth to 20.4 pmol/kg at 930 m (i.e., 5 m above the seafloor).

### 3.5. Pb and Nd Isotopic Compositions in Leachates and MUC Porewater

Due to insufficient quantities of available Nd in extracted porewater (below 0.2 ng at each depth), the Nd isotopic compositions in the porewaters were not analyzed. The recovered porewater Pb quantities are also low but Pb isotopic compositions from some depths could still be determined. We only compared $^{208}Pb/^{206}Pb$ in the porewater because $^{208}Pb$ and $^{206}Pb$ are the two most abundant Pb isotopes in nature, hence providing the best possible precision among all Pb isotopic ratios. As shown in Figure 8, the MUC bottom water Pb isotopic compositions (e.g. $^{206}Pb/^{204}Pb$ and $^{208}Pb/^{206}Pb$) at three stations are almost identical and very distinct from seawater Pb isotope signals in the water column above. The unradiogenic (low) $^{206}Pb/^{204}Pb$ of MUC

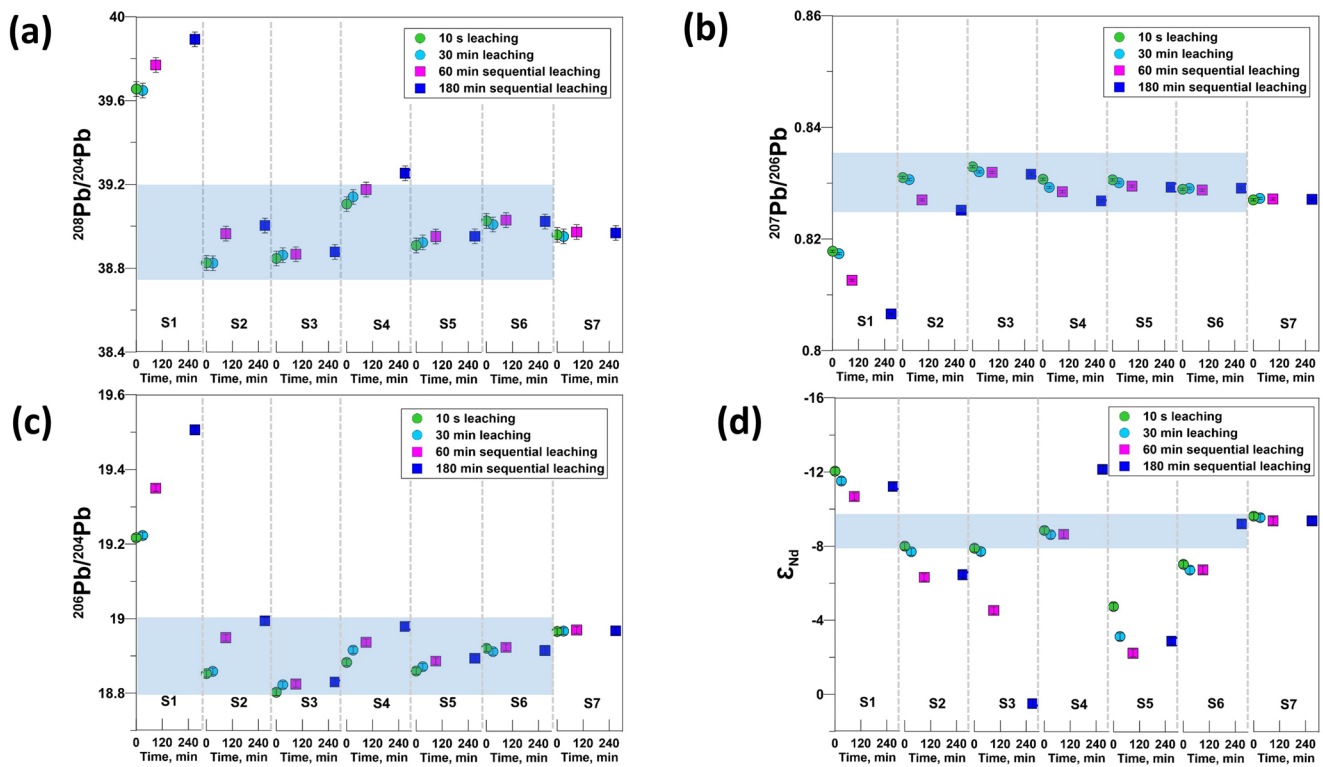**Figure 5.** Effect of leaching time on Pb and Nd isotopic compositions. (a) $^{208}Pb/^{204}Pb$, (b) $^{207}Pb/^{206}Pb$, (c) $^{206}Pb/^{204}Pb$, and (d) $\varepsilon_{Nd}$. The round symbols show results of quick 10-s leaching and 30-min conventional leaching, obtained separately with fresh samples. The square symbols show sequential leaching results carried out by mixing 30-min leaching residues with new leaching solution for 60 min (adding up to a total exposure time of 90 min), and again with renewed leaching solution for addition 180 min (adding up to a total exposure time of 270 min). The blue shades indicate the range of expected SO seawater Pb and Nd isotope signatures (Abouchami & Goldstein, 1995; Stichel, Frank, Rickli, & Haley, 2012).

bottom water indicate its origin is likely anthropogenic. We also noticed more than 10 times higher recovered Pb concentrations in MUC bottom water than in CTD seawater (Figure 7). The suspect MUC bottom water Pb isotopic signature is evidently overprinted by Pb contamination sourced from the MUC sampler itself because Pb bricks are used as a weight mounted on top of the MUC sampling tubes. The $^{208}Pb/^{206}Pb$ in the upper few centimeters within the sediment porewater also shifted toward the distinct Pb contamination signature seen in MUC bottom water, suggesting that Pb derived from the MUC weights also invaded the unconsolidated top centimeters of the sediment porefluids. However, the porewater $^{208}Pb/^{206}Pb$ below about 8 cm were resolvable not affected by this downcore Pb diffusion and agree with $^{208}Pb/^{206}Pb$ values in sediment leachates extracted using the 10-s leaching method. The CTD sampled shelf bottom water $^{208}Pb/^{206}Pb$ at our three sampled stations is consistently in the range of 2.066–2.071, which is only slightly offset from the core top leachate ($^{208}Pb/^{206}Pb$ = 2.055–2.061). Since the seawater sampling setup was not trace metal clean and recovered porewater Pb concentrations were very low, improved approaches in the future should lead to a better match between bottom water compositions and core top sediment leachates. These results demonstrate that authigenic Pb extracted from Weddell Sea shelf sediments using the improved reductive leaching approach reflect the porewater Pb isotope signal derived from bottom water.

The Nd concentrations in MUC bottom water samples, ranging from 20.9 to 27.6 pmol/kg (Figures 6b and Table S5), are slightly higher than the bottom water sampled by CTD several meters above, but only 3 liters of filtered seawater were recovered from each MUC station. The very low quantities of Nd recovered from MUC bottom water for Nd isotopic composition measurement resulted in highly expanded measurement uncertainties. The average MUC bottom water $\varepsilon_{Nd}$ value of $-8.9 \pm 2.4$ from these three stations, however, is identical to bottom seawater at all three stations. Similar to Pb, the average $\varepsilon_{Nd}$ extracted via reductive leaching from the top 10 cm of sediment are consistent in all three cores, ranging from $-8.4$ to $-8.6$ but are slightly offset overlying CTD seawater and MUC seawater $\varepsilon_{Nd}$ signature (Figure 8) on the order of 0.2–0.6 $\varepsilon_{Nd}$.
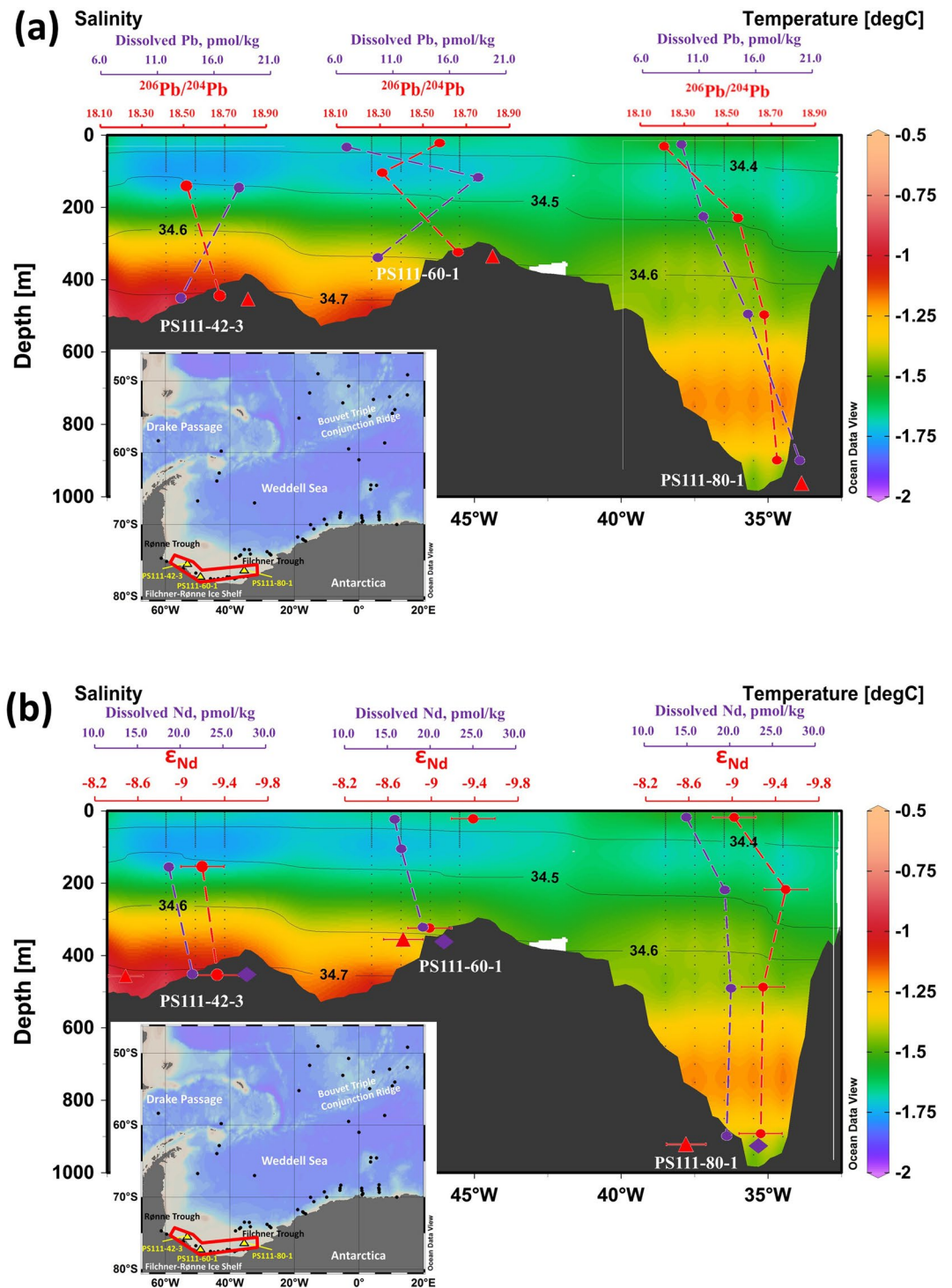
**Figure 6.** Concentrations and isotopic compositions of CTD-sampled seawater Pb and Nd with hydrological context in front of Filchner-Rønne Ice Shelf. (a) Pb data set; (b) Nd data set. Round dots indicate seawater data. The purple diamonds show Nd concentrations in MUC bottom water. The red triangles indicate authigenic isotopic compositions extracted from core top sediments at the first centimeter core depth. The transect (red line), locations of CTD&MUC station (yellow triangles) and used core top sediment (black dots) mentioned in the text are marked in the inlet map. Color-mapped seawater temperature, with salinity contours overlain, as drawn from the 2009 World Ocean Atlas (Zweng et al., 2013). MUC, multicore.
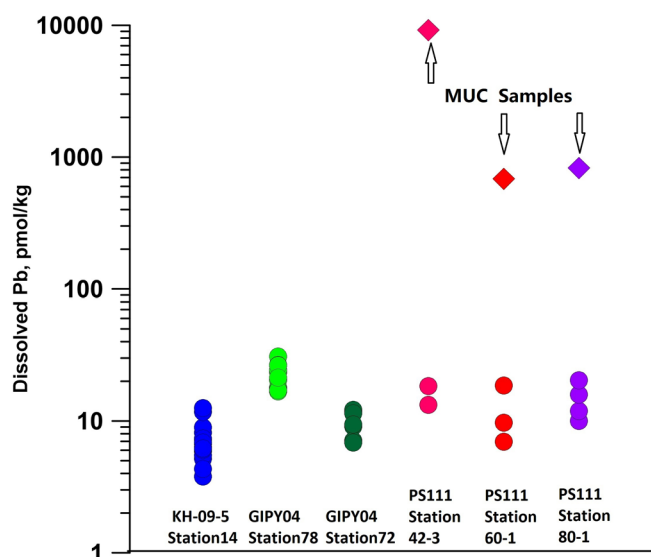
**Figure 7.** Comparison of seawater Pb concentrations collected from cruise PS111 and two close GEOTRACES stations (KH-09-5 and GIPY04). The seawater samples collected by CTD are marked by round dots and recovered by MUC are showed as diamonds. The seawater Pb concentration data of KH-09-5 (Lee et al., 2015) and GIPY04 (Schlitzer et al., 2018) were taken from the GEOTRACES database. MUC, multicore.

### 3.6. Authigenic Pb and Nd Isotopic Variability in the Atlantic Sector of the Southern Ocean

Figure 9 shows three different Pb isotope signature domains on the map: $^{206}Pb/^{204}Pb < 18.5$, $^{206}Pb/^{204}Pb > 19.0$ along the East Antarctic continental margin and other areas with an average Weddell Sea $^{206}Pb/^{204}Pb$ of about 18.8 (Abouchami & Goldstein, 1995). Authigenic $\varepsilon_{Nd}$ core top compositions also allow defining three areas which are slightly different from areas defined via $^{206}Pb/^{204}Pb$ (Figure 9b). Extracted $\varepsilon_{Nd}$ found to the east of the Drake Passage and in the northeast at the Bovet Triple Conjunction are more radiogenic than ambient seawater with $\varepsilon_{Nd} > -6$. Core top sediments near the East Antarctic continent have the most unradiogenic $\varepsilon_{Nd}$ ranging from $-10.3$ to $-12.5$, also deviating from regional bottom water compositions. The rest of the $\varepsilon_{Nd}$ values extracted from core top sediments agree with published seawater $\varepsilon_{Nd}$ signatures (Stichel, Frank, Rickli, & Haley, 2012).

## 4. Discussion

### 4.1. Seawater Pb and Nd on the Filchner-Rønne Shelf

The seawater Pb samples collected for this study were sampled by a standard CTD approach, which is not trace metal clean, so the samples were potentially contaminated to some extent. One indicator as to whether the sampled seawater Pb is contaminated is the dissolved Pb concentration, where substantially elevated Pb concentration values in the sample is a sign of contamination. Reported seawater Pb concentrations in the Atlantic sector of Southern Ocean from previous GEOTRACES cruises GA10 and GIPY04 are lower than 23 pmol/kg (Schlosser et al., 2019) and 31 pmol/kg (Schlitzer et al., 2018), respectively. Sampled Pb in all our seawater samples collected by CTD are below 21 pmol/kg (Figure 7), with minimum concentrations as low as 7 pmol/kg, indicating no significant contaminations, while the concentrations of the contaminated Pb samples collected via the separate MUC approach are on the order of 600 pmol/kg or higher. The seawater Pb isotopic composition is another important indicator for Pb contamination. Anthropogenic Pb usually has characteristically unradiogenic Pb isotopic signatures, i.e. low in $^{206}Pb/^{204}Pb$, $^{207}Pb/^{204}Pb$, and $^{208}Pb/^{204}Pb$ values (Bollhöfer & Rosman, 2000; Lee et al., 2015). As shown in Figure 6, the shelf bottom water $^{206}Pb/^{204}Pb$ ratios at these three stations are very consistently in the range from 18.65 to 18.72, which agree with recently reported Antarctic Bottom Water $^{206}Pb/^{204}Pb$ ratios of $18.68 \pm 0.06$ and $18.78 \pm 0.07$ in the Indian sector of Southern Ocean (Lee et al., 2015), suggesting that the Pb contamination from our standard CTD sampling process is minor or negligible.

The vertical seawater Nd concentrations in the studied three CTD stations (Figure 6b) increase with water depth. This pattern is similar to the general trend in the Weddell Sea (Stichel, Frank, Rickli, Hathorne, et al., 2012) and can be explained by reversible particle scavenging (Siddall et al., 2008; Stichel, Frank, Rickli, & Haley, 2012). A strong benthic flux was suggested to dominate seawater Nd isotope signatures near the continent in settings such as the eastern North Pacific (Abbott, Haley, & McManus, 2015; Abbott, Haley, McManus, 2015, & Reimers, (2015)) or deglacial deep Labrador Sea (Blaser et al., 2020). Analogously, such elevated fluxes may be expected at the Filchner-Rønne shelf given its proximal geological setting and high Ice Rafted Debris (IRD) contributions in the sediment. Strikingly, highly elevated bottom water Nd concentrations that were observed at various shelf locations in front of the West Antarctic Ice Sheet that were almost twice the concentration seen at similar water depths offshore (Carter et al., 2012; Rickli et al., 2014) are not found to be equally significant in the southernmost Weddell Sea (Figure 6b). In fact, the slightly higher Nd concentrations at depth are in agreement with the comparable water depth data in the open Weddell Sea, even though this may be a coincidence (Stichel, Frank, Rickli, & Haley, 2012). Overall, the relatively moderate bottom water Nd concentration on the Filchner-Rønne shelf suggests the contri-
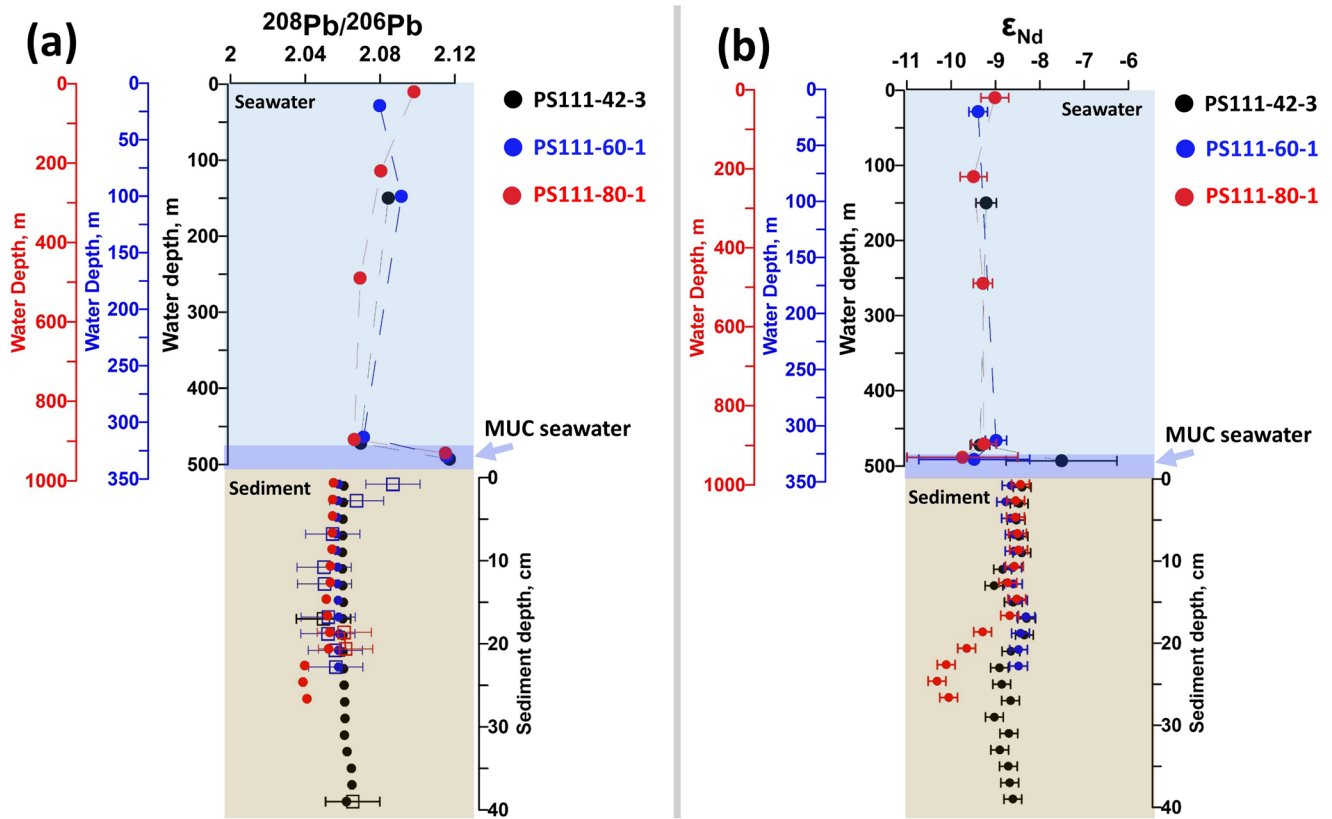
**Figure 8.** Pb and Nd isotopic compositions in CTD-sampled shelf seawater, MUC-sampled bottom water, porewater and leachates at three stations in front of Filchner-Rønne Ice Shelf (sample locations illustrated in Figure 1). (a) $^{208}$Pb/$^{206}$Pb and (b) $\varepsilon_{Nd}$. The round symbols in the seawater and sediment indicate seawater and leachate isotopic compositions. The empty square symbols indicate porewater $^{208}$Pb/$^{206}$Pb ratios. Different colored *y* axis is employed to indicate water depth of seawater samples from the three CTD stations, while only black *y* axis is used to show sediment depth. MUC, multicore.
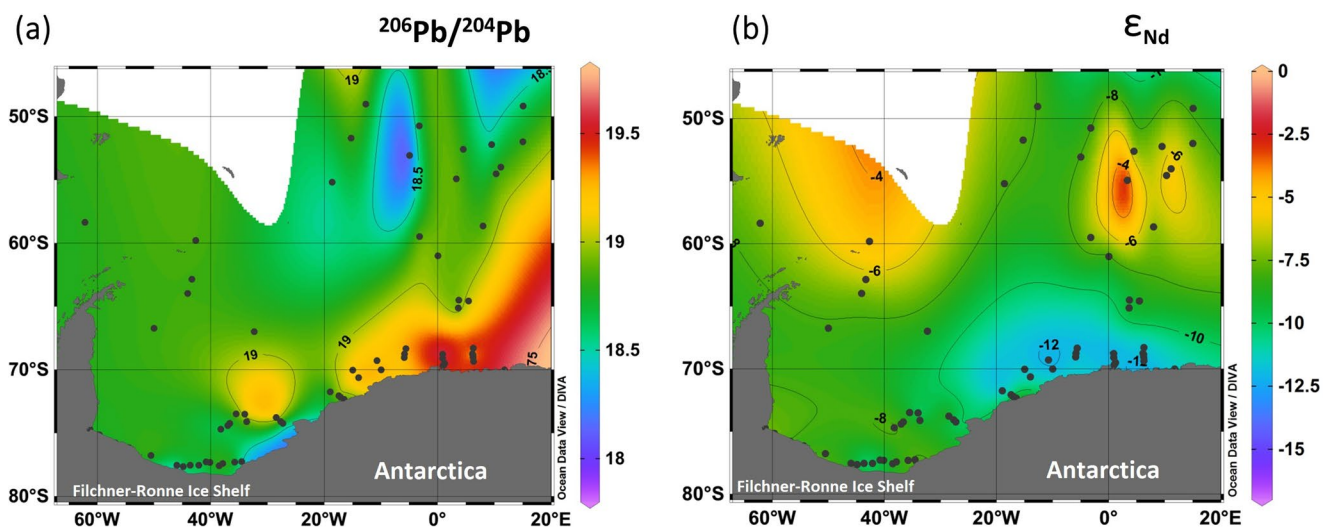


**Figure 9.** Authigenic $^{206}$Pb/$^{204}$Pb and $\varepsilon_{Nd}$ isotopic maps generated from core top sediments in the Atlantic sector of the Southern Ocean. (a) $^{206}$Pb/$^{204}$Pb and (b) $\varepsilon_{Nd}$.
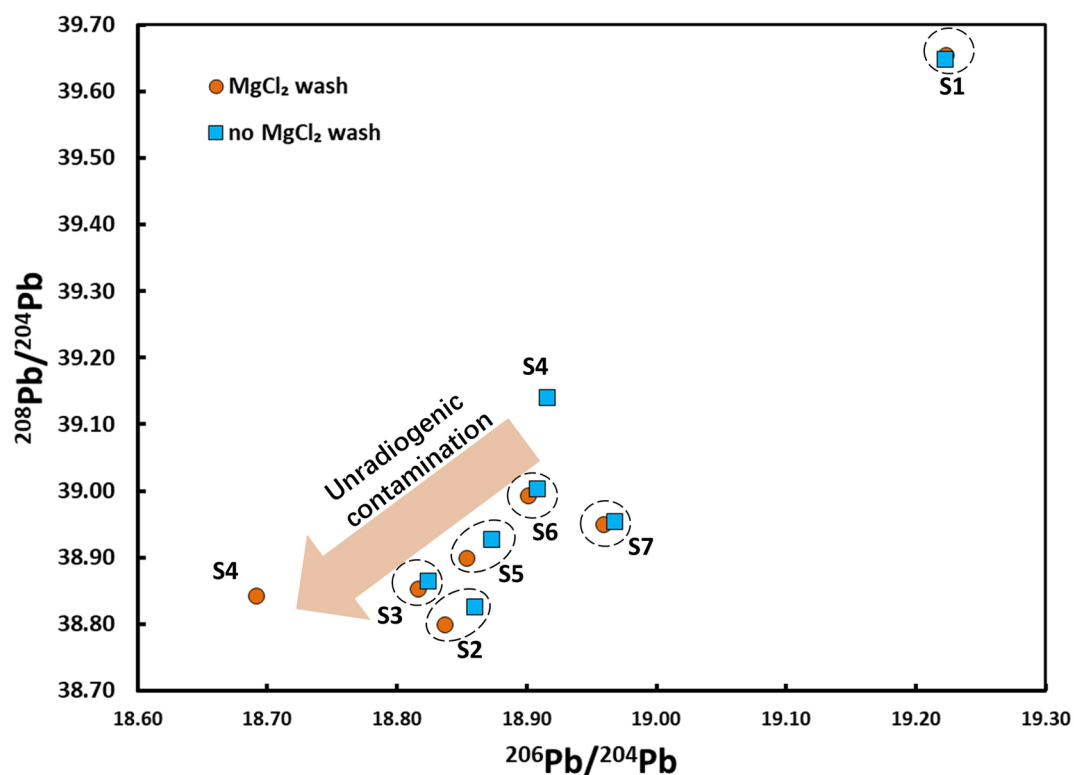
**Figure 10.** $MgCl_2$ pre-wash effects on Pb isotopic composition extracted from leaching test samples in $^{208}Pb/^{204}Pb$-$^{206}Pb/^{204}Pb$ spacing.

bution of Nd boundary additions to the Southern Ocean seawater Nd budget may vary in different regions around the Antarctic continental margin.

### 4.2. Measures for Reliable Porewater Pb and Nd Isotope Extraction from Southern Ocean Sediments

Most Pb isotope signals extracted from the samples pre-treated with $MgCl_2$ were shifted to less radiogenic Pb isotope compositions toward the same direction in $^{208}Pb/^{204}Pb$-$^{206}Pb/^{204}Pb$ space (Figure 10), with this contribution likely being of the anthropogenic origin from the same source. Because $MgCl_2$ solution is the only variable factor in this experiment, the external Pb contamination was most likely sourced from the $MgCl_2$ solution itself. As shown in Figures 3 and 10, samples with low authigenic Pb concentrations (S2–S5) are more affected due to relatively higher proportions of Pb contamination from $MgCl_2$ solution in the extracted aliquots. However, neither the most affected sample S4 featured the lowest concentration nor did the least affected sample S1 yield the highest concentration. As a result, the sample lithology should also play a role in the process as some samples may contain organic matter, which can preferentially absorb more Pb (Strawn & Sparks, 2000). Interestingly, we did not observe substantial changes in Pb concentration while the Pb isotopic composition clearly was altered. The process might take place under a solution-particle exchange equilibrium affecting only Pb isotope compositions but not concentrations, as seen in seawater (Wu et al., 2010). Background Nd concentrations in inorganic chemicals are commonly much lower than respective Pb contaminations, so neither Nd concentration nor isotopic compositions were altered by $MgCl_2$ pre-wash, which is similar to what has been found before (Haley et al., 2008). Since we found $MgCl_2$ to potentially introduce Pb contamination into the sample, while we conversely observed no significant improvement of extracted Nd signatures, we suggest avoiding the $MgCl_2$ pre-wash step preceding reductive leaching.

Previous leaching protocols that used EDTA required less than 1 g of sediment (Blaser et al., 2016; Gutjahr et al., 2007) but an alternative approach without ligands suggested using sometimes more than 10 grams of

sediment (Wilson et al., 2013). As shown in Figure 4, adding EDTA equally strongly prevents re-adsorption of Nd and we suggest using EDTA in the leaching solution in order to keep sediment usage at a minimum. One concern of using chelating ligands is that it may introduce contamination either from impurity of the chemical itself or by promoting solid phase dissolution reactions, e.g. DTPA can help to dissolve barites (Putnis et al., 2008). Since no significant isotopic changes were observed in our experiments under involvement of EDTA or DTPA, the contamination from impurity or contribution from side effect reactions appears negligible in the studied region. The only exception is mainly S4 in which Pb isotopic compositions in the leachates were shifted when using different ligands but $\varepsilon_{Nd}$ values remained identical. Re-adsorption of Pb is unlikely to cause such shifts in Pb isotopic composition since this offset was not observed in other samples when the re-adsorption effect was equally effective. One possible reason is that the sample was not perfectly homogenized. As shown in Figure 12, the leachate without ligands in S4 show lower Al/Pb and Al/Nd ratios than leachate with EDTA, while in the majority of the other samples the results are reversed. It indicates that the portion of the S4 sample used for leaching without ligands contains materials that released substantial extra quantities of Pb and Nd with altered Pb isotope signal but hydrogenetic Nd signature which could probably be fossil fish teeth (Basak et al., 2011). Although the ultimate reason for this effect cannot be resolved here, leaching with EDTA still resulted in $^{206}Pb/^{204}Pb$ compositions within the seawater signature range and in agreement with neighboring core top sediment sampling stations (Figure 9a) while $^{206}Pb/^{204}Pb$ are too low (<18.76) when using DTPA or no reductive the leaching solution without ligands.

One general observation from previous reductive leaching studies for Nd is that shorter leaching times appear to provide more reliable results since less non-authigenic sedimentary phases are effectively targeted during shorter exposure to the reductive solution (Blaser et al., 2016; Gourlan et al., 2010; Gutjahr et al., 2007; Wilson et al., 2013). Compared with the 10-s quick leaching approach, both Pb and Nd isotope signals extracted via the conventional 30-min leaching from separated sediment samples are always more radiogenic and closer to the subsequent one-hour sequential leaching signals which contained a higher proportion non-hydrogenetic Pb and Nd (Figure 5), indicating that a 10-s exposure to leaching acquired the purest hydrogenetic signals. Although the $\varepsilon_{Nd}$ in S5 and S6 even for samples with the shortest exposure time are offset by Nd additions from regional volcanic substrate in the sediment (Latimer et al., 2006), 10-s leaching still led to $\varepsilon_{Nd}$ values closer to actual seawater compositions (Figure 5d). A common reservation toward only leaching sediments for 10 s is that the Pb and Nd recovered may not be sufficient for isotope analysis. However, we found that this very short leaching approach recovered more or less the same amount of Pb and Nd as extracted during 30 min of leaching (Figure 11).

It has been found that Nd extracted from authigenic Fe-Mn oxyhydroxides via the reductive leaching method in many cases provides identical results to Nd extraction from sedimentary foraminifera, which in turn reflect the porewater origin of the Nd isotope signal (Blaser et al., 2016; Du et al., 2016). The porewater Nd isotope signal is derived from overlying seawater and sometimes modified by benthic exchange processes with the detrital phase (Abbott, Haley, & McManus, 2015). We also observed that the $\varepsilon_{Nd}$ values extracted using the 10-s leaching method from three MUC sediment cores provided compositions slightly offset from MUC to CTD seawater Nd isotope signature immediately above the sediment (Figure 8b) within 1 $\varepsilon_{Nd}$. The $\varepsilon_{Nd}$ deviation between porewater and overlying seawater is likely caused by release of Nd from IRD and/or clays in the sediment because these three MUC sediments are all dominantly muddy with substantial quantities of IRD present within. Previous studies showed that IRD (Blaser et al., 2019), poorly weathered material (Howe et al., 2016) and clays (Ohr et al., 1991) could all release Nd from the terrigenous fraction during early diagenesis.

Another important finding of this study is that the Pb isotope signal obtained via 10-s leaching of MUC sediments is identical to the porewater Pb isotope signal. Compositions are only slightly offset from bottom seawater Pb isotope signatures sampled via CTD (Figure 8a), although the latter may also be induced by the non-trace metal clean water sampling approach. Although it is generally assumed that the Pb isotope signature preserved in sedimentary authigenic Fe-Mn oxyhydroxides records a porewater signal, for the first time, this assumption could be validated by actual corresponding porewater Pb isotope compositions.
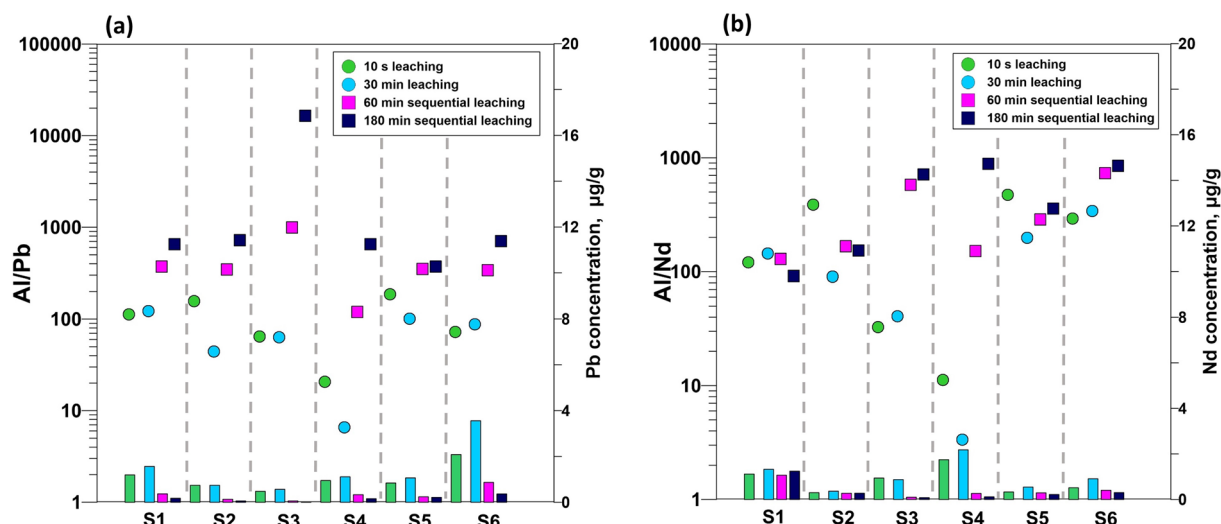
**Figure 11.** Variations of Al/Pb, Al/Nd, Pb and Nd concentrations of sediment samples during the sequential leaching. (a) Al/Pb and Pb concentration. (b) Al/Nd and Nd concentration. Green circle dots indicate Al/Pb or Al/Nd of 10-s leaching. Square dots indicate Al/Pb or Al/Nd of sequential leaching. Bar charts show extracted Pb and Nd concentrations.

### 4.3. Elemental Ratios as Proxies for Non-hydrogenetic Contamination

Elemental ratios in reductive Fe-Mn oxyhydroxide leachate solutions were previously used as proxies for monitoring non-hydrogenetic contamination: 1) REE patterns for the origin of Nd (Bayon et al., 2002; Martin et al., 2010); 2) Al/Pb and Al/Nd for non-hydrogenetic phases (Gutjahr et al., 2007). REE patterns were not investigated in this study because these were recently shown to be unreliable for the identification of contaminating phases in certain sedimentary settings (Blaser et al., 2016). Al/Pb and Al/Nd ratios were used to monitor dissolution of the detrital and potentially present volcanogenic fraction, due to high Al/Pb and Al/Nd ratios in non-hydrogenetic phases and low ratios in hydrogenetic phases (Blaser et al., 2016; Gutjahr et al., 2007). However, care should be taken to compare like with like. If the degree of re-adsorption affects or even dominates the concentration for highly particle reactive elements, the application of this proxy may be limited and the Al/Pb and Al/Nd ratios then only reflect the different re-adsorption behavior of Al, Pb, and Nd. As shown during the tests constraining the efficiency of chelating ligands, the extracted Pb and Nd isotopic compositions were identical in individual samples (Figure 4) but the Al/Pb and Al/Nd (Figure 12) fluctuated dramatically, i.e. Al/Pb of S7 ranged from 10 to 10,000. Leaching without EDTA, in most cases, led to high Al/Pb and Al/Nd, indicating more Pb and Nd were re-adsorbed during reductive dissolution of the Fe-Mn oxyhydroxide phase.

When EDTA was used to prevent re-adsorption during leaching, Al/Pb and Al/Nd worked well in sequential leaching tests with exposure times from 30 min to 270 min (Figure 11a and 11b). For example, the Nd isotope signals in S5 and S6 were offset by volcanogenic contributions leading to high Al/Nd (cf. Blaser et al., 2016). Moreover, the $\varepsilon_{Nd}$ values in 30 min sediment leachates (S2, S3, and S6) are consistent with seawater $\varepsilon_{Nd}$ yielding Al/Nd lower than 100, which is similar to a threshold ratio for good quality Nd isotope data found in previous studies (Blaser et al., 2016; Gutjahr et al., 2007). However, the 10-s leaching method did not always result in lower Al/Pb and Al/Nd than 30 min leaching, although 10-s leaching extracted a purer hydrogenetic Pb and Nd portion from the bulk sediments as indicated by the respective isotopic compositions. More specifically, 10-s and 30-min leaching on S2 recovered comparable quantities of Pb and Nd, but 10-s leaching extracted more Al than 30-min leaching, resulting in high Al/Pb and Al/Nd ratios. The reason for this difference is likely related to pH change since $Al^{3+}$ in the solution starts to precipitate at pH = 3.7 and almost quantitatively precipitates at pH = 4.7. The 30-min leaching consumed more acetic acid than the 10-s exposure approach which elevates solution pH in the former, therefore precipitating more Al prior to extraction of the supernatant. These considerations reveal that the elemental behavior during leaching can be complex so that the interpretation based on
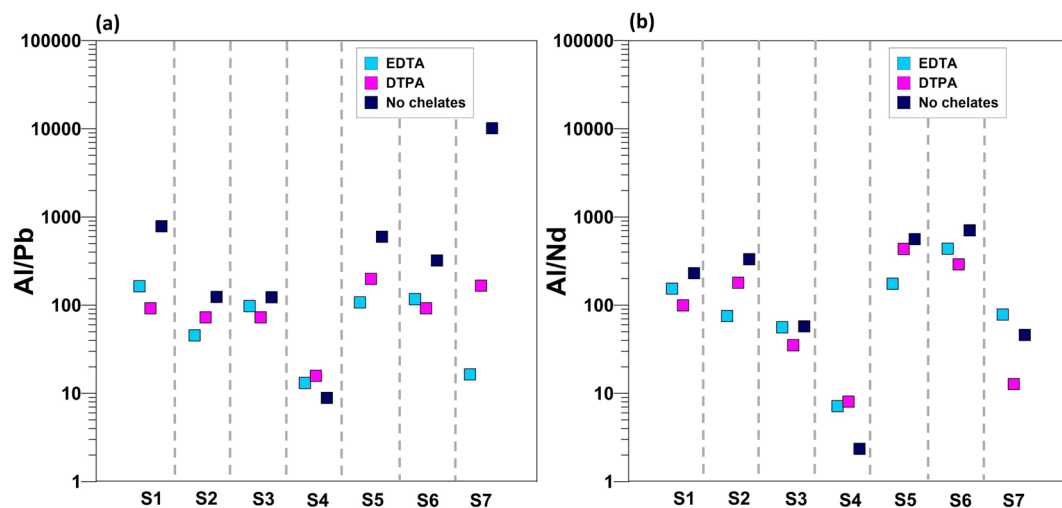
**Figure 12.** Variations of Al/Pb and Al/Nd of all samples using different ligands in the leaching solution. (a) Al/Pb. (b) Al/Nd.

elemental concentrations and ratios should be made very carefully, even though in the large majority of cases in our experiments the low Al/Pb and Al/Nd ratio (<100) indicated reliable hydrogenetic Pb and Nd extraction.

### 4.4. Identifying Sampling Areas for SO-wide Palaeocirculation Reconstructions Away from Localized Antarctic Depocenters

Although 10-s leaching can ideally selectively mobilize Pb and Nd from sedimentary Fe-Mn oxyhydroxides with minimal contributions from non-hydrogenetic phases during leaching, the Pb and Nd preserved in sedimentary Fe-Mn oxyhydroxides phase may not always be of seawater origin. If authigenic Fe-Mn oxyhydroxides were for example containing continental pre-formed Fe-Mn oxyhydroxides (Bayon et al., 2004; Kraft et al., 2013; F. Pöppelmeier et al., 2018) and/or imprinted local porewater signal released from terrigenous (Blaser et al., 2019; Du et al., 2016; F. Pöppelmeier et al., 2018) and volcanic materials (Blaser et al., 2016; Elmore et al., 2011) during early diagenesis, reductive leaching inevitably dissolved these alongside the ambient seawater-derived fraction because these are chemically the same. For instance, 10-s leaching was not able to extract a seawater Pb isotopic signal from S1 and seawater Nd isotopic signals from S1, S5, and S6 (Figure 5). There is still no ideal solution to overcome the intrinsic limitation of reductive leaching, but those disturbing sedimentary effects seems to only occur in specific geological settings as shown in Figure 9.

First, our data revealed that both $^{206}Pb/^{204}Pb$ (>19.0) and $\varepsilon_{Nd}$ (from −10.3 to −12.5) extracted from core top sediments near the East Antarctic continent are offset from nearby seawater $\varepsilon_{Nd}$ and Pb isotope signatures reported from surface scrapings of Fe-Mn nodules (Abouchami & Goldstein, 1995). These could be caused by partially dissolving continental detritus or/and pre-formed ferromanganese coatings during leaching. Partial dissolution of detrital components in the sediment should lead to high Al/Pb and Al/Nd ratios in the leachates (Blaser et al., 2016; Gutjahr et al., 2007), but the Al/Pb and Al/Nd ratios of the 10-s S1 leachate (Figure 11) are low, indicating that our leaching approach did not significantly target the detrital fraction. Therefore, regionally or locally supplied continental Pb and Nd isotope signatures in pre-formed Fe-Mn oxyhydroxides likely overprinted both extracted seawater-derived Pb and Nd from authigenic Fe-Mn oxyhydroxides in sediments near the Antarctic continental margin. The pre-formed Fe-Mn oxyhydroxides in the study area could for example be supplied by nearby ice streams (Rignot et al., 2011) or be associated with sinking organic matter. Recent studies postulated such an effect of temporarily elevated pre-formed Fe-Mn oxyhydroxide delivery with bottom currents for example in the abyssal NW Atlantic (Howe et al., 2016; F. Pöppelmeier et al., 2018; Jaume-Seguí et al., 2020).

Second, the extracted $\varepsilon_{Nd}$ from sediments located to the east of Drake Passage and in the Bouvet Triple Conjunction ridge display very radiogenic (high) values compared with ambient deep water compositions due to Nd release from volcanic components within the sediments from nearby volcanic sources (Stichel, Frank, Rickli, Hathorne, et al., 2012). The elevated Al/Nd ratios in S5 and S6 (Figures 11b) also point toward contributions of volcanic material. Interestingly, Pb in S5 and S6 10-s leachates seems to be unaffected by volcanic contributions as we did not observe equally elevated Al/Pb in samples S5 and S6 (Figures 11a). Furthermore, $^{206}Pb/^{204}Pb$ extracted from sediments in the area enriched in volcanic materials area did not display compositions offset from expected seawater signals (Abouchami & Goldstein, 1995). Taken together, these observations suggest that the extraction of authigenic Pb may be less susceptible to analytically introduced artefacts than seen for authigenic Nd.

Although extracted Pb is apparently relatively robust against contamination by sedimentary volcanic material, anthropogenic Pb contributions supplied by dust can alter the natural seawater signal. Pb extracted from core top sediments in the northeast of the research area closest to South Africa are extremely altered by anthropogenic Pb contamination (Figure 9a). The lack of sea ice protection and relative proximity to the African continent could both result in the strong anthropogenic Pb footprint in these surface sediments, because winter sea ice does not extend that far north and Pb sourced from Africa was found in nearby water masses (Paul, van de Flierdt, et al., 2015). As shown in Figure 8a, the artificial dissolved Pb released from Pb sampling weight only penetrated the topmost few centimeters in the sediment. Although this is not an equal modern anthropogenic oceanic process, it indicates that the extracted downcore Pb isotope signals in the lower parts should not be affected. Overall, the sedimentary Fe-Mn oxyhydroxides in core sites located in the open ocean, which are far away from Antarctica and volcanically active regions (green color area in Figure 9), generally preserve credible seawater Pb and Nd isotope signals.

## 5. Conclusions

We developed a fast 10-s leaching method to extract authigenic Pb and Nd isotope signatures from Southern Ocean sediments and validated this method by directly comparing the Pb and Nd isotope signal in sediment leachates with overlying seawater Nd and Pb isotopic signatures and corresponding Pb porewater compositions. Utilizing the 10-s leaching method established in this study, we screened core top sediments in the Atlantic sector of Southern Ocean for their hydrogenetic Pb and Nd isotope distribution in order to identify suitable sediment core sites for future paleoceanographic reconstructions.

The use of a previously employed sedimentary pre-leaching cleaning technique using $MgCl_2$ was evaluated. Furthermore, the effect of using or omitting chelate ligands was assessed, and the optimal leaching time was determined. Our data show that the $MgCl_2$ wash is not necessary and, on the other hand, may potentially contaminate the authigenic Pb isotope signature in sedimentary samples. Experiments to constrain the effect of chelating ligands were carried out by two commonly used ligands, EDTA and DTPA. Adding the chelating ligands during leaching was confirmed to be very important for leaching. When the leaching process was carried out without ligands, both Pb and Nd were substantially re-adsorbed in the sediment. Between these two ligands, EDTA most efficiently prevented re-adsorption both for Pb and Nd, while no mass fractionation or contamination was observed. Moreover, the sequential leaching test indicated that the very short 10-s leaching approach extracted the purest hydrogenetic Pb and Nd signatures in all tested sediment samples and recovered sufficient quantities of Pb and Nd for isotope analysis. Therefore, we recommend using the 10-s leaching method in combination with EDTA to extract hydrogenetic Pb and Nd in Southern Ocean sediments.

The analysis of Pb and Nd isotope seawater signatures and porewater Pb isotopic compositions demonstrated that the extracted hydrogenetic Pb and Nd by 10-s leaching in our settings reflect the porewater isotope signals which may, however, in places be slightly offset from ambient seawater signal due to early diagenetic porewater processes.

The previously suggested leaching quality assessment proxies, Al/Nd and Al/Pb, also provide a critical insight regarding the nature of the extracted phase for Southern Ocean sediments when EDTA is present during leaching. The low Al/Nd and Al/Pb ratios (<100) in our experiments reflect the predominant extraction of a Fe-Mn oxyhydroxide phase but the high Al/Nd and Al/Pb ratios did not necessarily reflect tapping of

the detrital phase since slow pH increase during longer leaching unavoidably induces Al precipitation and complex re-adsorption reactions.

We expect the 10-s leaching approach also to work in sediments from other marine settings, but this technique should be tested before the application on downcore reconstructions. If strong benthic flux and/or pre-formed continentally derived ferromanganese oxyhydroxides present, the extracted seawater Pb and Nd isotopic signals are highly likely compromised, which ultimately can be ascribed to the limitation of the paleoceanographic archive. As a general guide, 1) the extracted Pb and Nd isotopic compositions from core top sediments must at least agree with overlying bottom water signals; 2) suitable core sites should be further away from continental margins to prevent input of significant pre-formed ferromanganese oxyhydroxides; 3) as stated earlier, in the case of authigenic Nd, the sediment core should contain no or only minute quantities of volcanic material.

## Data Availability Statement

Metadata and other results from the sediment cores, porewater, and seawater are available within supporting information and the Pangaea data base (DOI: https://doi.pangaea.de/10.1594/PANGAEA.924604). Constructive criticism provided by three anonymous reviewers helped improving an earlier version of the manuscript and is greatly acknowledged. Editorial handling by Branwen Williams is appreciated.

## References

Abbott, A. N., Haley, B. A., & McManus, J. (2015). Bottoms up: Sedimentary control of the deep North Pacific Ocean's ε$_{Nd}$ signature. *Geology*, *43*(11), 1035.

Abbott, A. N., Haley, B. A., McManus, J., & Reimers, C. E. (2015). The sedimentary flux of dissolved rare earth elements to the ocean. *Geochimica et Cosmochimica Acta*, *154*, 186–200.

Abouchami, W., & Goldstein, S. L. (1995). A lead isotopic study of circum-antarctic manganese nodules. *Geochimica et Cosmochimica Acta*, *59*(9), 1809–1820.

Abouchami, W., Goldstein, S. L., Gazer, S. J. G., Eisenhauer, A., & Mangini, A. (1997). Secular changes of lead and neodymium in central Pacific seawater recorded by a Fe-Mn crust. *Geochimica et Cosmochimica Acta*, *61*(18), 3957–3974.

Arsouze, T., Dutay, J. C., Lacan, F., & Jeandel, C. (2009). Reconstructing the Nd oceanic cycle using a coupled dynamical-biogeochemical model. *Biogeosciences*, *6*(12), 2829–2846.

Baker, J., Peate, D., Waight, T., & Meyzen, C. (2004). Pb isotopic analysis of standards and samples using a 207Pb–204Pb double spike and thallium to correct for mass bias with a double-focusing MC-ICP-MS. *Chemical Geology*, *211*(3), 275–303.

Basak, C., Martin, E. E., & Kamenov, G. D. (2011). Seawater Pb isotopes extracted from Cenozoic marine sediments. *Chemical Geology*, *286*(3), 94–108.

Bayon, G., German, C. R., Boella, R. M., Milton, J. A., Taylor, R. N., & Nesbitt, R. W. (2002). An improved method for extracting marine sediment fractions and its application to Sr and Nd isotopic analysis. *Chemical Geology*, *187*(3), 179–199.

Bayon, G., German, C. R., Burton, K. W., Nesbitt, R. W., & Rogers, N. (2004). Sedimentary Fe–Mn oxyhydroxides as paleoceanographic archives and the role of aeolian flux in regulating oceanic dissolved REE. *Earth and Planetary Science Letters*, *224*(3), 477–492.

Belshaw, N. S., Freedman, P. A., O'Nions, R. K., Frank, M., & Guo, Y. (1998). A new variable dispersion double-focusing plasma mass spectrometer with performance illustrated for Pb isotopes. *International Journal of Mass Spectrometry*, *181*(1), 51–58.

Blaser, P., Gutjahr, M., Pöppelmeier, F., Frank, M., Kaboth-Bahr, S., & Lippold, J. (2020). Labrador Sea bottom water provenance and REE exchange during the past 35,000 years. *Earth and Planetary Science Letters*, *542*, 116299.

Blaser, P., Lippold, J., Gutjahr, M., Frank, N., Link, J. M., & Frank, M. (2016). Extracting foraminiferal seawater Nd isotope signatures from bulk deep sea sediment by chemical leaching. *Chemical Geology*, *439*, 189–204.

Blaser, P., Pöppelmeier, F., Schulz, H., Gutjahr, M., Frank, M., Lippold, J., et al. (2019). The resilience and sensitivity of Northeast Atlantic deep water ε$_{Nd}$ to overprinting by detrital fluxes over the past 30,000 years. *Geochimica et Cosmochimica Acta*, *245*, 79–97.

Bollhöfer, A., & Rosman, K. J. R. (2000). Isotopic source signatures for atmospheric lead: The Southern Hemisphere. *Geochimica Et Cosmochimica Acta*, *64*(19), 3251–3262.

Burton, K. W., Ling, H.-F., & O'Nions, R. K. (1997). Closure of the Central American Isthmus and its effect on deep-water formation in the North Atlantic. *Nature*, *386*(6623), 382–385.

Carter, P., Vance, D., Hillenbrand, C. D., Smith, J. A., & Shoosmith, D. R. (2012). The neodymium isotopic composition of waters masses in the eastern Pacific sector of the Southern Ocean. *Geochimica et Cosmochimica Acta*, *79*, 41–59.

Chen, T.-Y., Frank, M., Haley, B. A., Gutjahr, M., & Spielhagen, R. F. (2012). Variations of North Atlantic inflow to the central Arctic Ocean over the last 14 million years inferred from hafnium and neodymium isotopes. *Earth and Planetary Science Letters*, *353–354*, 82–92.

Chester, R., & Hughes, M. J. (1967). A chemical technique for the separation of Ferro-manganese minerals, carbonate minerals and adsorbed trace elements from pelagic sediments. *Chemical Geology*, *2*, 249–262.

Christensen, J. N., Halliday, A. N., Godfrey, L. V., Hein, J. R., & Rea, D. K. (1997). Climate and ocean dynamics and the lead isotopic records in Pacific ferromanganese crusts. *Science*, *277*(5328), 913–918.

Cochran, J. K., McKibbin-Vaughan, T., Dornblaser, M. M., Hirschberg, D., Livingston, H. D., & Buesseler, K. O. (1990). 210Pb scavenging in the North Atlantic and North Pacific Oceans. *Earth and Planetary Science Letters*, *97*(3), 332–352.

Cohen, A. S., O'Nions, R. K., Siegenthaler, R., & Griffin, W. L. (1988). Chronology of the pressure-temperature history recorded by a granulite terrain. *Contributions to Mineralogy and Petrology*, *98*(3), 303–311.

Colin, C., Frank, N., Copard, K., & Douville, E. (2010). Neodymium isotopic composition of deep-sea corals from the NE Atlantic: Implications for past hydrological changes during the Holocene. *Quaternary Science Reviews*, *29*(19), 2509–2517.

Crocket, K. C., Foster, G. L., Vance, D., Richards, D. A., & Tranter, M. (2013). A Pb isotope tracer of ocean-ice sheet interaction: the record from the NE Atlantic during the Last Glacial/Interglacial cycle. *Quaternary Science Reviews*, *82*, 133–144.

Crocket, K. C., Vance, D., Foster, G. L., Richards, D. A., & Tranter, M. (2012). Continental weathering fluxes during the last glacial/interglacial cycle: insights from the marine sedimentary Pb isotope record at Orphan Knoll, NW Atlantic. *Quaternary Science Reviews*, *38*, 89–99.

Diekmann, B., Fütterer, D. K., Grobe, H., Hillenbrand, C.-D., Kuhn, G., Michels, K., et al. (2003). *Ice rafted debris distribution in 16 sediment cores from the South Atlantic*, PANGAEA. Retrieved from https://doi.org/10.1594/PANGAEA.732965

Diekmann, B., & Kuhn, G. (1999). Provenance and dispersal of glacial-marine surface sediments in the Weddell Sea and adjoining areas, Antarctica: ice-rafting versus current transport. *Marine Geology*, *158*(1), 209–231.

Du, J., Haley, B. A., & Mix, A. C. (2016). Neodymium isotopes in authigenic phases, bottom waters and detrital sediments in the Gulf of Alaska and their implications for paleo-circulation reconstruction. *Geochimica et Cosmochimica Acta*, *193*, 14–35.

Elmore, A. C., Piotrowski, A. M., Wright, J. D., & Scrivner, A. E. (2011). Testing the extraction of past seawater Nd isotopic composition from North Atlantic deep sea sediments and foraminifera. *Geochemistry, Geophysics, Geosystems*, *12*(9), Q09008. https://doi.org/10.1029/2011GC003741

Foster, G. L., & Vance, D. (2006). Negligible glacial–interglacial variation in continental chemical weathering rates. *Nature*, *444*(7121), 918–921.

Frank, M. (2002). Radiogenic isotopes: Tracers of past ocean circulation and erosional input. *Reviews of Geophysics*, *40*(1), 1–38. https://doi.org/10.1029/2000RG000094

Frank, M., Whiteley, N., Kasten, S., Hein, J. R., & O'Nions, K. (2002). North Atlantic deep water export to the Southern Ocean over the past 14 Myr: Evidence from Nd and Pb isotopes in ferromanganese crusts. *Paleoceanography*, *17*(2) 1–9. https://doi.org/10.1029/2000PA000606

Gourlan, A. T., Meynadier, L., Allègre, C. J., Tapponnier, P., Birck, J.-L., & Joron, J.-L. (2010). Northern Hemisphere climate control of the Bengali rivers discharge during the past 4 Ma. *Quaternary Science Reviews*, *29*(19), 2484–2498.

Gutjahr, M., Frank, M., Halliday, A. N., & Keigwin, L. D. (2009). Retreat of the Laurentide ice sheet tracked by the isotopic composition of Pb in western North Atlantic seawater during termination 1. *Earth and Planetary Science Letters*, *286*(3–4), 546–555.

Gutjahr, M., Frank, M., Stirling, C. H., Klemm, V., van de Flierdt, T., & Halliday, A. N. (2007). Reliable extraction of a deepwater trace metal isotope signal from Fe–Mn oxyhydroxide coatings of marine sediments. *Chemical Geology*, *242*(3), 351–370.

Haley, B. A., Frank, M., Spielhagen, R. F., & Fietzke, J. (2008). Radiogenic isotope record of Arctic Ocean circulation and weathering inputs of the past 15 million years. *Paleoceanography*, *23*(1), PA1S13. https://doi.org/10.1029/2007PA001486

Haley, B. A., Klinkhammer, G. P., & McManus, J. (2004). Rare earth elements in pore waters of marine sediments. *Geochimica et Cosmochimica Acta*, *68*(6), 1265–1279.

Hathorne, E. C., Haley, B., Stichel, T., Grasse, P., Zieringer, M., & Frank, M. (2012). Online preconcentration ICP-MS analysis of rare earth elements in seawater. *Geochemistry, Geophysics, Geosystems*, *13*(1), Q01020. https://doi.org/10.1029/2011GC003907

Henderson, G. M., & Maier-Reimer, E. (2002). Advection and removal of 210Pb and stable Pb isotopes in the oceans: A general circulation model study. *Geochimica et Cosmochimica Acta*, *66*(2), 257–272.

Howe, J. N. W., Piotrowski, A. M., & Rennie, V. C. F. (2016). Abyssal origin for the early Holocene pulse of unradiogenic neodymium isotopes in Atlantic seawater. *Geology*, *44*(10), 831–834.

Huang, H., Gutjahr, M., Eisenhauer, A., & Kuhn, G. (2020). No detectable Weddell Sea Antarctic bottom water export during the last and penultimate glacial maximum. *Nature Communications*, *11*(1), 424.

Jaume-Seguí, M., Kim, J., Pena, L. D., Goldstein, S. L., Knudson, K. P., Yehudai, M., et al. (2020). Distinguishing glacial AMOC and interglacial non-AMOC Nd isotopic signals in the deep western Atlantic over the last 1 Myr. *Paleoceanography and Paleoclimatology*, *36*, e2020PA003877. https://doi.org/10.1029/2020PA003877

Klevenz, V., Vance, D., Schmidt, D. N., & Mezger, K. (2008). Neodymium isotopes in benthic foraminifera: Core-top systematics and a down-core record from the Neogene south Atlantic. *Earth and Planetary Science Letters*, *265*(3), 571–587.

Kraft, S., Frank, M., Hathorne, E. C., & Weldeab, S. (2013). Assessment of seawater Nd isotope signatures extracted from foraminiferal shells and authigenic phases of Gulf of Guinea sediments. *Geochimica et Cosmochimica Acta*, *121*, 414–435.

Kurzweil, F., Gutjahr, M., Vance, D., & Keigwin, L. (2010). Authigenic Pb isotopes from the Laurentian Fan: Changes in chemical weathering and patterns of North American freshwater runoff during the last deglaciation. *Earth and Planetary Science Letters*, *299*(3), 458–465.

Lacan, F., & Jeandel, C. (2005). Neodymium isotopes as a new tool for quantifying exchange fluxes at the continent–ocean interface. *Earth and Planetary Science Letters*, *232*(3), 245–257.

Lacan, F., Tachikawa, K., & Jeandel, C. (2012). Neodymium isotopic composition of the oceans: A compilation of seawater data. *Chemical Geology*, *300–301*, 177–184.

Latimer, J. C., Filippelli, G. M., Hendy, I. L., Gleason, J. D., & Blum, J. D. (2006). Glacial-interglacial terrigenous provenance in the southeastern Atlantic Ocean: The importance of deep-water sources and surface currents. *Geology*, *34*(7), 545–548.

Lee, J.-M., Boyle, E. A., Gamo, T., Obata, H., Norisuye, K., & Echegoyen, Y. (2015). Impact of anthropogenic Pb and ocean circulation on the recent distribution of Pb isotopes in the Indian Ocean. *Geochimica et Cosmochimica Acta*, *170*, 126–144.

Lee, J.-M., Boyle, E. A., Suci Nurhati, I., Pfeiffer, M., Meltzner, A. J., & Suwargadi, B. (2014). Coral-based history of lead and lead isotopes of the surface Indian Ocean since the mid-20th century. *Earth and Planetary Science Letters*, *398*, 37–47.

Lee, J.-M., Eltgroth, S. F., Boyle, E. A., & Adkins, J. F. (2017). The transfer of bomb radiocarbon and anthropogenic lead to the deep North Atlantic Ocean observed from a deep sea coral. *Earth and Planetary Science Letters*, *458*, 223–232.

Lugmair, G. W., & Galer, S. J. G. (1992). Age and isotopic relationships among the angrites Lewis Cliff 86010 and Angra dos Reis. *Geochimica et Cosmochimica Acta*, *56*(4), 1673–1694.

Martin, E. E., Blair, S. W., Kamenov, G. D., Scher, H. D., Bourbon, E., Basak, C., et al. (2010). Extraction of Nd isotopes from bulk deep sea sediments for paleoceanographic studies on Cenozoic time scales. *Chemical Geology*, *269*(3), 414–431.

Martin, E. E., & Scher, H. D. (2004). Preservation of seawater Sr and Nd isotopes in fossil fish teeth: Bad news and good news. *Earth and Planetary Science Letters*, *220*(1), 25–39.

Michels, K., Kuhn, G., Hillenbrand, C.-D., Diekmann, B., Fütterer, D. K., Grobe, H., et al. (2002). *Grain size composition of sediment cores from the Weddell Sea, Antarctica*, PANGAEA. Retrieved from https://doi.org/10.1594/PANGAEA.472241

Middelburg, J. J., van der Weijden, C. H., & Woittiez, J. R. W. (1988). Chemical processes affecting the mobility of major, minor and trace elements during weathering of granitic rocks. *Chemical Geology*, *68*(3), 253–273.

Ndungu, K., Zurbrick, C. M., Stammerjohn, S., Severmann, S., Sherrell, R. M., & Flegal, A. R. (2016). Lead sources to the Amundsen Sea, West Antarctica. *Environmental Science & Technology*, *50*(12), 6233–6239.

O'Nions, R. K., Frank, M., von Blanckenburg, F., & Ling, H. F. (1998). Secular variation of Nd and Pb isotopes in ferromanganese crusts from the Atlantic, Indian and Pacific Oceans. *Earth and Planetary Science Letters*, *155*(1), 15–28.

Ohr, M., Halliday, A. N., & Peacor, D. R. (1991). Sr and Nd isotopic evidence for punctuated clay diagenesis, Texas Gulf Coast. *Earth and Planetary Science Letters*, *105*(1), 110–126.

Paul, M., Bridgestock, L., Rehkämper, M., van DeFlierdt, T., & Weiss, D. (2015). High-precision measurements of seawater Pb isotope compositions by double spike thermal ionization mass spectrometry. *Analytica Chimica Acta*, *863*, 59–69.

Paul, M., van de Flierdt, T., Rehkämper, M., Khondoker, R., Weiss, D., Lohan, M. C., et al. (2015). Tracing the Agulhas leakage with lead isotopes. *Geophysical Research Letters*, *42*(20), 8515–8521. https://doi.org/10.1002/2015GL065625

Pearce, C. R., Jones, M. T., Oelkers, E. H., Pradoux, C., & Jeandel, C. (2013). The effect of particulate dissolution on the neodymium (Nd) isotope and rare Earth element (REE) composition of seawater. *Earth and Planetary Science Letters*, *369–370*, 138–147.

Pöppelmeier, F., Gutjahr, M., Blaser, P., Keigwin, L. D., & Lippold, J. (2018). Origin of Abyssal NW Atlantic water masses since the last glacial maximum. *Paleoceanography and Paleoclimatology*, *33*(5), 530–543. https://doi.org/10.1029/2017PA003290

Pöppelmeier, F., Scheen, J., Blaser, P., Lippold, J., Gutjahr, M., & Stocker, T. F. (2020). Influence of elevated Nd fluxes on the northern Nd isotope end member of the Atlantic during the early holocene. *Paleoceanography and Paleoclimatology*, *35*(11), e2020PA003973. https://doi.org/10.1029/2020PA003973

Putnis, C. V., Kowacz, M., & Putnis, A. (2008). The mechanism and kinetics of DTPA-promoted dissolution of barite. *Applied Geochemistry*, *23*(9), 2778–2788.

Rempfer, J., Stocker, T. F., Joos, F., Dutay, J.-C., & Siddall, M. (2011). Modelling Nd-isotopes with a coarse resolution ocean circulation model: Sensitivities to model parameters and source/sink distributions. *Geochimica et Cosmochimica Acta*, *75*(20), 5927–5950.

Reynolds, B. C., Frank, M., & O'Nions, R. K. (1999). Nd- and Pb-isotope time series from Atlantic ferromanganese crusts: implications for changes in provenance and paleocirculation over the last 8 Myr. *Earth and Planetary Science Letters*, *173*(4), 381–396.

Rickli, J., Gutjahr, M., Vance, D., Fischer-Gödde, M., Hillenbrand, C.-D., & Kuhn, G. (2014). Neodymium and hafnium boundary contributions to seawater along the West Antarctic continental margin. *Earth and Planetary Science Letters*, *394*, 99–110.

Rignot, E., Mouginot, J., & Scheuchl, B. (2011). Ice flow of the Antarctic Ice sheet. *Science*, *333*(6048), 1427–1430.

Rijkenberg, M. J. A., de Baar, H. J. W., Bakker, K., Gerringa, L. J. A., Keijzer, E., Laan, M., et al. (2015). "PRISTINE", a new high volume sampler for ultraclean sampling of trace metals and isotopes. *Marine Chemistry*, *177*, 501–509.

Roberts, N. L., Piotrowski, A. M., McManus, J. F., & Keigwin, L. D. (2010). Synchronous deglacial overturning and water mass source changes. *Science*, *327*(5961), 75–78.

Schaule, B. K., & Patterson, C. C. (1981). Lead concentrations in the northeast Pacific: Evidence for global anthropogenic perturbations. *Earth and Planetary Science Letters*, *54*(1), 97–116.

Schlitzer, R., Anderson, R. F., Dodas, E. M., Lohan, M., Geibert, W., Tagliabue, A., et al. (2018). The GEOTRACES intermediate data product 2017. *Chemical Geology*, *493*, 210–223.

Schlosser, C., Karstensen, J., & Woodward, E. M. S. (2019). Distribution of dissolved and leachable particulate Pb in the water column along the GEOTRACES section GA10 in the South Atlantic. *Deep Sea Research Part I: Oceanographic Research Papers*, *148*, 132–142.

Siddall, M., Khatiwala, S., van de Flierdt, T., Jones, K., Goldstein, S. L., Hemming, S., et al. (2008). Towards explaining the Nd paradox using reversible scavenging in an ocean general circulation model. *Earth and Planetary Science Letters*, *274*(3), 448–461.

Staudigel, H., Doyle, P., & Zindler, A. (1985). Sr and Nd isotope systematics in fish teeth. *Earth and Planetary Science Letters*, *76*(1), 45–56.

Stichel, T., Frank, M., Rickli, J., & Haley, B. A. (2012). The hafnium and neodymium isotope composition of seawater in the Atlantic sector of the Southern Ocean. *Earth and Planetary Science Letters*, *317–318*, 282–294.

Stichel, T., Frank, M., Rickli, J., Hathorne, E. C., Haley, B. A., Jeandel, C., et al. (2012). Sources and input mechanisms of hafnium and neodymium in surface waters of the Atlantic sector of the Southern Ocean. *Geochimica et Cosmochimica Acta*, *94*, 22–37.

Strawn, D. G., & Sparks, D. L. (2000). Effects of soil organic matter on the kinetics and mechanisms of Pb(II) sorption and desorption in soil. *Soil Science Society of America Journal*, *64*(1), 144–156.

Struve, T., van de Flierdt, T., Burke, A., Robinson, L. F., Hammond, S. J., Crocket, K. C., et al. (2017). Neodymium isotopes and concentrations in aragonitic scleractinian cold-water coral skeletons—Modern calibration and evaluation of palaeo-applications. *Chemical Geology*, *453*, 146–168.

Süfke, F., Gutjahr, M., Gilli, A., Anselmetti, F. S., Glur, L., & Eisenhauer, A. (2019). Early stage weathering systematics of Pb and Nd isotopes derived from a high-Alpine Holocene lake sediment record. *Chemical Geology*, *507*, 42–53.

Tachikawa, K., Athias, V., & Jeandel, C. (2003). Neodymium budget in the modern ocean and paleo-oceanographic implications. *Journal of Geophysical Research*, *108*(C8), 3254. https://doi.org/10.1029/1999JC000285

Tachikawa, K., Jeandel, C., & Roy-Barman, M. (1999). A new approach to the Nd residence time in the ocean: The role of atmospheric inputs. *Earth and Planetary Science Letters*, *170*(4), 433–446.

Tanaka, T., Togashi, S., Kamioka, H., Amakawa, H., Kagami, H., Hamamoto, T., et al. (2000). JNdi-1: A neodymium isotopic reference in consistency with LaJolla neodymium. *Chemical Geology*, *168*(3), 279–281.

Tessier, A., Campbell, P. G. C., & Bisson, M. (1979). Sequential extraction procedure for the speciation of particulate trace metals. *Analytical Chemistry*, *51*(7), 844–851.

Thirlwall, M. F. (2002). Multicollector ICP-MS analysis of Pb isotopes using a 207Pb-204Pb double spike demonstrates up to 400 ppm/amu systematic errors in Tl-normalization. *Chemical Geology*, *184*(3), 255–279.

van de Flierdt, T., Frank, M., Halliday, A. N., Hein, J. R., Hattendorf, B., Günther, D., et al. (2004). Deep and bottom water export from the Southern Ocean to the Pacific over the past 38 million years. *Paleoceanography*, *19*(1), PA1020. https://doi.org/10.1029/2003PA000923

van de Flierdt, T., Pahnke, K., Amakawa, H., Andersson, P., Basak, C., Coles, B., et al. (2012). GEOTRACES intercalibration of neodymium isotopes and rare earth element concentrations in seawater and suspended particles. Part 1: reproducibility of results for the international intercomparison. *Limnology and Oceanography: Methods*, *10*(4), 234–251.

van de Flierdt, T., Robinson, L. F., Adkins, J. F., Hemming, S. R., & Goldstein, S. L. (2006). Temporal stability of the neodymium isotope signature of the Holocene to glacial North Atlantic. *Paleoceanography*, *21*(4), PA4102. https://doi.org/10.1029/2006PA001294

Vance, D., & Burton, K. (1999). Neodymium isotopes in planktonic foraminifera: a record of the response of continental weathering and ocean circulation rates to climate change. *Earth and Planetary Science Letters*, *173*(4), 365–379.

Vance, D., & Thirlwall, M. (2002). An assessment of mass discrimination in MC-ICPMS using Nd isotopes. *Chemical Geology*, *185*(3–4), 227–240.

Wilson, D. J., Crocket, K. C., van de Flierdt, T., Robinson, L. F., & Adkins, J. F. (2014). Dynamic intermediate ocean circulation in the North Atlantic during Heinrich Stadial 1: A radiocarbon and neodymium isotope perspective. *Paleoceanography*, *29*(11), 1072–1093. https://doi.org/10.1002/2014PA002674

Wilson, D. J., Piotrowski, A. M., Galy, A., & Clegg, J. A. (2013). Reactivity of neodymium carriers in deep sea sediments: Implications for boundary exchange and paleoceanography. *Geochimica et Cosmochimica Acta*, *109*, 197–221.

Wilson, D. J., van de Flierdt, T., & Adkins, J. F. (2017). Lead isotopes in deep-sea coral skeletons: Ground-truthing and a first deglacial Southern Ocean record. *Geochimica et Cosmochimica Acta*, *204*, 350–374.

Wu, J., Rember, R., Jin, M., Boyle, E. A., & Flegal, A. R. (2010). Isotopic evidence for the source of lead in the North Pacific abyssal water. *Geochimica et Cosmochimica Acta*, *74*(16), 4629–4638.

Yusoff, Z. M., Ngwenya, B. T., & Parsons, I. (2013). Mobility and fractionation of REEs during deep weathering of geochemically contrasting granites in a tropical setting, Malaysia. *Chemical Geology*, *349–350*, 71–86.

Zweng, M. M., Reagan, J. R., Antonov, J. I., Locarnini, R. A., Mishonov, A. V., Boyer, T. P., et al. (2013). Salinity. *World Ocean Atlas*, *2013*, 2.